Genetic evidence for Amh modulation of gonadotropin actions to control gonadal homeostasis and gametogenesis in zebrafish and its noncanonical signalling through Bmpr2a receptor

Zhiwei Zhang, Kun Wu, Zhiqin Ren, Wei Ge*

Centre of Reproduction, Development and Aging (CRDA), Faculty of Health Sciences, University of Macau, Taipa, Macau, China

Key words: anti-Müllerian hormone; gonadal development; folliculogenesis; spermatogenesis; zebrafish

Conflict of Interest: The authors declare no conflict of interest.

**Corresponding author*:

Wei Ge, Faculty of Health Sciences, University of Macau, Taipa, Macau, China;

Tel: +853-8822-4996; Email: weige@um.edu.mo/gezebrafish@gmail.com

Abstract

Anti-Müllerian hormone (AMH/Amh) plays an important role in gonadal function. Amh deficiency caused severe gonadal dysgenesis and dysfunction in zebrafish with gonadal hypertrophy in both sexes. However, its action mechanism remains unknown. Intriguingly, the Amh cognate type II receptor (Amhr2) is missing in the zebrafish genome, in sharp contrast to other species. Using a series of zebrafish mutants (*amh*, *fshb*, *fshr* and *lhcgr*), we provided unequivocal evidence for Amh actions via modulating gonadotropin signaling on both germ cell proliferation and differentiation. The gonadal hypertrophy in *amh* mutants was abolished in the absence of FSH receptor (Fshr) in females or Fshr/LH receptor (Lhcgr) in males. Furthermore, we demonstrated that knockout of bone morphogenetic protein (BMP) type II receptor A (*bmpr2a*), but not *bmpr2b*, phenocopied all phenotypes of *amh* mutant in both sexes, including gonadal hypertrophy, hyper-proliferation of germ cells, retarded gametogenesis and reduced *fshb* expression. In summary, the present study provided comprehensive genetic evidence for an intimate interaction of gonadotropin and Amh pathways in gonadal homeostasis and gametogenesis and for Bmpr2a as the possible missing link for Amh signaling in zebrafish.

Introduction

Anti-Müllerian hormone (AMH/Amh), also named Müllerian-inhibiting substance (MIS), is a distant member of the transforming growth factor-β (TGF-β) superfamily (Josso and di Clemente, 1999), and its primary function is to induce Müllerian duct regression in mammals during sex differentiation (Behringer et al., 1994; Vigier et al., 1984). In addition, AMH also plays important roles in gonadal development and function (Durlinger et al., 2002; Rehman et al., 2017; Visser et al., 2007; Visser and Themmen, 2005). As AMH is primarily produced in early follicles, its serum level has been used as a major indicator for testing ovarian reserve in clinic (Broer et al., 2014), and abnormal expression of AMH has been considered one of the factors associated with primary ovarian insufficiency (POI) or premature ovarian failure (POF) (Monniaux et al., 2014; Visser et al., 2012) and polycystic ovarian syndrome (PCOS) (Barbotin et al., 2019; Garg and Tal, 2016; Pigny et al., 2003). In mice, knockout of AMH gene led to increased ovarian weight and accelerated recruitment of primordial follicles (Durlinger et al., 1999); however, the number of preovulatory follicles remained relatively constant in AMH null mice, and this was attributed to an increased atresia, which neutralized the increased number of preantral follicles recruited from the primordial follicle pool (Visser et al., 2007). In teleosts, recent studies from us and others showed that disruption of Amh gene in zebrafish (Lin et al., 2017; Yan et al., 2019; Zhang et al., 2020) and tilapia (Liu et al., 2019) resulted in gonadal hypertrophy due to increased proliferation of early germ cells and decreased differentiation. However, the mechanisms by which Amh works remain largely unknown.

Like other TGF-β family members, AMH signals through a specific type II receptor, AMHRII (Mishina et al., 1996). In humans, mutation of either AMH or AMHRII leads to persistence of the uterus and oviduct in males, which are functionally normal in reproduction (Josso et al., 2005). In mice, knockout of AMH had no effect on gonadal differentiation; however, the AMH-deficient males developed reproductive tract systems of both sexes including uterus and oviduct (Behringer et al., 1994). The same phenotypes were also observed in AMHRII null male mice (Mishina et al., 1996). Amh type II receptor (Amhr2) also exists in teleosts (Kluver et al., 2007), and an Amhr2 mutant (*hotei*) was identified by mutant screening and characterized in medaka

(Morinaga et al., 2007). The Amhr2 mutant medaka showed significant phenotypic abnormalities, including excessive proliferation of germ cells in both sexes and arrest of folliculogenesis at primary growth (PG) stage at 6 mph (months after hatching) (Morinaga et al., 2007). Further evidence showed that Amh primarily affected the germ cells undergoing mitotic self-renewal, but not the quiescent germ cells (Nakamura et al., 2012). The phenotypes of *amhr2* mutant medaka were similar to those of *amh* mutants in the zebrafish (Lin et al., 2017; Yan et al., 2019; Zhang et al., 2020). However, bioinformatics analysis has failed to identify any Amhr2 homologues in the zebrafish genome (Morinaga et al., 2007; Yan et al., 2019). How does Amh work in the zebrafish without its cognate type II receptor?

Using CRISPR/Cas9 approach, we undertook this study to investigate the downstream mechanisms by which Amh works in zebrafish gonads. Our data support previous reports on roles of Amh in zebrafish and medaka gametogenesis. More importantly, in combination with the mutant lines for gonadotropin receptors (*fshr* and *lhcgr*), we provided strong evidence for interactions of gonadotrophic and Amh signaling pathways in both ovary and testis. Furthermore, we also provided strong evidence that the bone morphogenetic protein (BMP) type II A receptor (Bmpr2a/*bmpr2a*) may most likely serve as the putative Amh type II receptor in zebrafish in the absence of its cognate Amhr2 receptor.

Results

Gonadal dysgenesis of amh mutant involves gonadotropin signaling

Using CRISPR/Cas9 method, we generated an indel mutation (+66, -4) in exon I of the *amh* gene, leading to frameshift mutation of *amh* gene (Zhang et al., 2020). As reported recently in zebrafish (Lin et al., 2017; Yan et al., 2019; Zhang et al., 2020), disruption of *amh* gene resulted in severe gonadal hypertrophy and blockade of gametogenesis in both sexes, in particular the testis, and both mutant ovaries and testes showed increased germ cell proliferation (PG follicles in the ovary and spermatogonia in the testis) ($amh^{-/-};fshb^{+/-}$ vs. $amh^{+/-};fshb^{+/-}$) but decreased germ cell differentiation, viz. meiosis in the testis and PG-PV transition in the ovary (Fig. 1). To investigate the mechanism by which Amh works, we focused our attention to pituitary gonadotropins,

especially follicle-stimulating hormone (FSH), because FSH plays an important role in promoting ovarian and testis growth in zebrafish (Zhang et al., 2015b). In mammalian models, AMH has been reported to stimulate pituitary FSH expression and secretion (Barbotin et al., 2019; Garrel et al., 2016; Kadokawa, 2020) but suppress gonadal responsiveness to FSH (Durlinger et al., 2001; Visser and Themmen, 2014).

To address this issue, we first created an *amh* and *fshb* double mutant (*amh*$^{-/-}$;*fshb*$^{-/-}$) with the aim to demonstrate how pituitary FSH was involved in the phenotypic abnormalities of *amh* mutant. Surprisingly, we did not see any significant effect of FSH deficiency on phenotypic abnormalities in both females and males of *amh* mutant at 4 mpf (*amh*$^{-/-}$;*fshb*$^{-/-}$ vs. *amh*$^{-/-}$;*fshb*$^{+/-}$) (Fig. 1). Since the role of FSH in promoting gonadal growth could be taken up by LH after puberty in *fshb* null mutant (Zhang et al., 2015b), we hypothesized that the lack of influence of FSH deficiency on adult *amh* mutant could be due to the compensatory effect of LH for FSH as both gonadotropins can activate FSH receptor (Fshr) in the zebrafish (So et al., 2005; Zhang et al., 2015b).

To test this hypothesis, we then created double and triple knockouts involving *amh* and the two gonadotropin receptors (*fshr* and *lhcgr*). Our recent study showed that the loss of *fshr* caused hypotrophy of the ovary and complete arrest of folliculogenesis at early PG stage without significant effect on spermatogenesis in mature adults, whereas double knockout of *fshr* and *lhcgr* led to complete arrest of spermatogenesis in early stage (Zhang et al., 2015a). Based on these, we designed an experiment by creating *amh* and *fshr* double knockout (*amh*$^{-/-}$;*fshr*$^{-/-}$) to look at the ovary and triple knockout (*amh*$^{-/-}$;*fshr*$^{-/-}$;*lhcgr*$^{-/-}$) to look at the testis. Analysis of these mutants with different gene combinations provided critical insights into the interactions of gonadotropin and Amh signaling pathways in controlling both germ cell proliferation (accumulation of PG follicles in the ovary and spermatogonia in the testis) and differentiation (PG-PV transition or follicle activation in the ovary and meiosis in the testis).

In females, the loss of Fshr in *amh* and *fshr* double mutant (*amh*$^{-/-}$;*fshr*$^{-/-}$) completely abolished the ovarian hypertrophy induced by *amh* deficiency with all follicles arrested at the PG stage as seen in *fshr* single mutant (*amh*$^{+/-}$;*fshr*$^{-/-}$). Comparing *amh* mutant in the presence or absence of *fshr* (*amh*$^{-/-}$;*fshr*$^{+/-}$ and *amh*$^{-/-}$;*fshr*$^{-/-}$), we could see clearly that the ovarian hypertrophy occurred only in the presence of

fshr. Interestingly, the accumulation of PG follicles in the hypertrophic *amh*$^{-/-}$;*fshr*$^{+/-}$ ovary was accompanied by reduced exit of PG follicles to advanced stage or PG-PV transition. Full-scaled folliculogenesis took place only when both *amh* and *fshr* were present as seen in the control (*amh*$^{+/-}$;*fshr*$^{+/-}$) (Fig. 2A).

Similar patterns were observed for testis development. The lack of both gonadotropin receptors *fshr/lhcgr* abolished testicular hypertrophy induced by *amh* mutation (*amh*$^{-/-}$;*fshr*$^{-/-}$;*lhcgr*$^{-/-}$), resulting in extremely underdeveloped testis with spermatogonia only as seen in *fshr/lhcgr* double mutant (*amh*$^{+/-}$;*fshr*$^{-/-}$;*lhcgr*$^{-/-}$). The testicular hypertrophy occurred only in the presence of *fshr/lhcgr* (*amh*$^{-/-}$;*fshr*$^{+/-}$;*lhcgr*$^{+/-}$) but with very limited meiotic entry. Like that in the ovary, normal testis size and full-scaled spermatogenesis happened only in the presence of all three genes (*amh*$^{+/-}$;*fshr*$^{+/-}$;*lhcgr*$^{+/-}$) (Fig. 2B).

Loss of bmpr2a phenocopies amh mutant in controlling gametogenesis

One intriguing issue about Amh actions in zebrafish is that there is no Amh type II receptor (Amhr2/*amhr2*) in its genome, in sharp contrast to other species including fish (Kluver et al., 2007; Liu et al., 2019; Morinaga et al., 2007). How does Amh signal then? Our hypothesis is that without its cognate type II receptor, Amh in zebrafish may signal through a related receptor of TGF-β receptor family, and the most possible candidate would be BMP type II receptor (Bmpr2) according to their phylogenetic relationship with Amhr2 (Fig. S1A). To address this issue, we created a *bmpr2a* mutant line with 5 base deletion (*bmpr2a*$^{-5/-5}$) (Fig. S1B). Phenotype analysis showed that the female mutant (*bmpr2a*$^{-/-}$) was similar to the controls (+/+ and +/-) in gross morphology including body weight and body length; however, the mutant showed an obviously expanded abdomen and significantly higher gonadosomatic index (GSI, gonad weight/body weight) at 5 mpf (Fig. 3A, C). Histological analysis of the ovaries revealed normal folliculogenesis in control females (+/+ and +/-) with all stages of follicles from primary growth (PG) to full-grown (FG) stages. In contrast, there was an enormous accumulation of follicles in the mutant ovaries (-/-) with most being at PG stage and very few follicles beyond previtellogenic (PV) stage (Fig. 3A), remarkably similar to the phenotype manifested by the age-matched *amh* mutant (Fig. 1A and 2A). As for males, the *bmpr2a* mutant (-/-) showed much larger belly with enormous size of testis compared to the male controls (+/+ and +/-) (Fig. 3B and C), which was again identical

to that of *amh* mutant males at the same stage (Fig. 1B and 2B). Histological analysis showed much abundant spermatogonia in mutant testes with limited meiosis (Fig. 3B). Other than gonadal hypertrophy and dysfunction, the *bmpr2a* mutant did not show much difference in sex ratio compared with the controls (Fig. 3D), again similar to *amh* mutant (Zhang et al., 2020).

Further evidence for Bmpr2a as putative Amh type II receptor in zebrafish

As suggested by the above result, Amh in zebrafish may signal through Bmpr2a in the absence of its cognate Amhr2 because the mutants of *amh* and *bmpr2a* phenocopied each other in terms of gonadal development and gametogenesis in both sexes. To further test this hypothesis, we generated an *amh* and *bmpr2a* double mutant ($amh^{-/-};bmpr2a^{-/-}$). At 3 mpf, both single mutants of *amh* ($amh^{-/-};bmpr2a^{+/-}$) and *bmpr2a* ($amh^{+/-};bmpr2a^{-/-}$) showed similar abnormality in folliculogenesis with accumulation of PG follicles (Fig. 4A). Interestingly, the ovary of the double mutant ($amh^{-/-};bmpr2a^{-/-}$) was comparable to those of *amh* and *bmpr2a* single mutants without any visible additive effects, and the ovarian weights as indicated by GSI were also comparable among three genotypes (Fig. 4C).

Similar to females, the males of all three genotypes, including single mutants of *amh* ($amh^{-/-};bmpr2a^{+/-}$) and *bmpr2a* ($amh^{+/-};bmpr2a^{-/-}$) as well as their double mutant ($amh^{-/-};bmpr2a^{-/-}$), showed the same phenotypes, including enormous testis hypertrophy with accumulation of spermatogonia and decreased entry into meiosis (Fig. 4B). Similar to females, the weights of testes (GSI) were also comparable among the three mutant groups, but they were all much higher than that in the control (Fig. 4C). Both males and females of the double mutant ($amh^{-/-};bmpr2a^{-/-}$) were sub-fertile at young age and able to produce viable offspring (Fig. 4D).

In addition to gonadal development, the *bmpr2a* mutant also phenocopied *amh* mutant in terms of *fshb* expression in the pituitary. As we reported recently, the expression of *fshb* in adult *amh* mutant males decreased dramatically (Zhang et al., 2020). As shown in Fig. 4E, the expression of *fshb* also decreased significantly in both *bmpr2a* single mutant and double mutant with *amh* (($amh^{-/-};bmpr2a^{-/-}$) (Fig. 4E).

Deficiency of bmpr2b leads to defective folliculogenesis in the ovary

Due to genome duplication in teleosts, genes in zebrafish often have duplicated copies. In addition to *bmpr2a*, zebrafish also has a duplicated copy of Bmpr2 gene (*bmpr2b*) (Fig. S1A). To evaluate the roles of *bmpr2b*, we also generated a mutant line with a 14-base insertion (*bmpr2b*$^{+14/+14}$) (Fig. S1B). In contrast to *bmpr2a*, the loss of *bmpr2b* had no effect on male development at 3 mpf and the mutant males (*bmpr2b*$^{-/-}$) showed normal body shape and testis morphology with normal fertility. Further histological analysis revealed normal process of spermatogenesis in the mutant (Fig. 5A).

In contrast to males, the *bmpr2b*-deficient females showed severe reproductive defects at 3 mpf. Histological analysis showed that despite comparable morphology at 3 mpf, the follicles in the mutant ovaries (*bmpr2b*$^{-/-}$) were much smaller than those in the control ovaries (+/+ and +/-), maximally to mid-vitellogenic (MV) stage (Fig. 5B). The follicles from the controls ranged from 150 μm to 700 μm, indicating normal folliculogenesis. In contrast, the follicles in *bmpr2b* mutant ovary ranged from 150 μm to maximally 400 μm only (Fig. 5C), suggesting an arrest of follicle growth at EV and/or MV stage, which have average diameters around 350 and 450 μm respectively (Zhou et al., 2011). The folliculogenesis in the mutant ovary remained arrested at 5 mpf (Fig. 5B), and most of the leading follicles exhibited atretic structures such as granulosa cell hypertrophy and abnormal chorion (Fig. 5D). To confirm the malfunction of the mutant females, we tested their fertility. The mutant females (*bmpr2b*$^{-/-}$) could only ovulate dozens of eggs each time during mating, in contrast to hundreds by control siblings (Fig. 6A), and the ovulated eggs from the mutant females were less than 550 μm in diameter, much smaller than those from the controls (about 750 μm) (Fig. 6B). All eggs from the mutant females could not undergo normal cleavage and died eventually, indicating failed fertilization; therefore, the *bmpr2b* mutant females were infertile (Fig. 6A and B).

Loss of Bmpr2 signaling results in juvenile mortality

Considering the importance of BMP signaling in animal development and severe early embryonic lethality in BMPRII null mice (Beppu et al., 2000), we were surprised by the lack of significant developmental defects in Bmpr2 single mutants except

reproduction (*bmpr2a*$^{-/-}$ and *bmpr2b*$^{-/-}$). To further address this issue, we generated Bmpr2-deficient double mutant (*bmpr2a*$^{-/-}$;*bmpr2b*$^{-/-}$). The double mutant could develop normally till 15 dpf, but died progressively afterwards. Most individuals died before 60 dpf with only a few survivors, indicating importance of Bmpr2 signaling for post-embryonic development. Details of developmental defects and potential cause of death are described in the supplemental materials (Fig. S2-4) (Supplemental Figures and Tables). Due to the high juvenile mortality and low vitality of the survivors, it was difficult to obtain sexually mature double mutants for analysis of reproductive performance.

Discussion

AMH was first identified for its inducing Müllerian duct regression during male differentiation (Behringer et al., 1994). Further studies have shown that it is also involved in controlling gonadal development and gametogenesis in both males and females (Durlinger et al., 2002; Rehman et al., 2017; Visser and Themmen, 2005). Interestingly, Amh/*amh* is also present in teleosts, which do not have Müllerian ducts (Pfennig et al., 2015). Genetic analyses in fish species have provided evidence for its primary roles in gonadal development and function. Disruption of Amh gene in zebrafish led to gonadal hypertrophy (Lin et al., 2017; Yan et al., 2019; Zhang et al., 2020), which is confirmed in the present study. Similarly, mutation of both Amh and Amhr2 in tilapia also resulted in ovarian hypertrophy and accumulation of PG follicles (Liu et al., 2019). These results agree well with the report in medaka on Amhr2 mutant (*hotei*) (Morinaga et al., 2007). Despite these studies, the action mechanisms of Amh still remain largely unknown in fish. More intriguingly, zebrafish does not even have the cognate type II receptor for Amh (Amhr2) (Morinaga et al., 2007; Yan et al., 2019). In this study, we provided genetic evidence for Amh modulation of gonadotropin signaling in controlling gonadal homeostasis and gametogenesis, specifically at the points of germ cell proliferation and differentiation. Furthermore, we also presented evidence that Amh in zebrafish may most likely signal through a noncanonical pathway involving BMP type II receptor A (Bmpr2a/*bmpr2a*), but not Bmpr2b/*bmpr2b*.

Interaction of gonadotropin and Amh signaling pathways in controlling germ cell proliferation and differentiation

As reported by others in different models, we also demonstrated that the lack of Amh significantly increased germ cell proliferation but decreased their differentiation in zebrafish. The increased germ cell proliferation resulted in accumulation of PG follicles in the ovary and spermatogonia in the testis, whereas their decreased differentiation was manifested by reduced exit of PG follicles to PV stage (follicle activation) in *amh* mutant ovary and limited meiotic entry to spermatocytes in the testis. The enormous growth of *amh* mutant gonads was therefore due to hyper-proliferation of the germ cells and their limited differentiation to advanced stages. Considering that pituitary gonadotropins are the master hormones that control gonadal growth and development and that AMH stimulates FSH expression and secretion (Barbotin et al., 2019; Garrel et al., 2016; Kadokawa, 2020) but suppresses gonadal sensitivity or responsiveness to FSH (Durlinger et al., 2001; Visser and Themmen, 2014), we hypothesized that the enormous growth of *amh* mutant gonads might involve gonadotropin signaling. As we reported recently, the loss of FSH (*fshb*) or its receptor (*fshr*) resulted in a significant suppression of gonadal growth and gametogenesis (Zhang et al., 2015a; Zhang et al., 2015b). However, the loss of *fshb* showed no impact on gonadal hypertrophy in adult *amh* mutant (*amh*$^{-/-}$;*fshb*$^{-/-}$). This could be due to the rescue of the lost FSH function by LH through Fshr at high concentrations (So et al., 2005). To test this hypothesis, we went on to generate double and triple mutants of *amh* and gonadotropin receptors (*fshr* and *lhcgr*). Interestingly, the loss of *fshr* completely abolished the phenotype of ovarian hypertrophy in female *amh* mutant (*amh*$^{-/-}$;*fshr*$^{-/-}$) and the loss of *fshr*/*lhcgr* abolished testicular hypertrophy in male *amh* mutant (*amh*$^{-/-}$;*fshr*$^{-/-}$;*lhcgr*$^{-/-}$). These results strongly suggest that Amh may act in the ovary and testis by suppressing gonadal responsiveness to gonadotropins. The loss of Amh would lead to over-activation of gonadotropin signaling by FSH and/or LH, resulting in increased generation of PG follicles in the ovary and proliferation of spermatogonia in the testis (Fig. 7). The inhibition of gonadotropin signaling, especially FSH, by AMH has also been reported in mammals (Durlinger et al., 2001; Visser and Themmen, 2005; Visser and Themmen, 2014). AMH reduced the sensitivity of ovarian follicles to FSH in mice as evidenced by an inhibitory effect of AMH on FSH-stimulated follicle growth *in vitro* (Durlinger et al., 2001), and this inhibition was partly due to reduced expression of

aromatase and FSHR (Grossman et al., 2008; Pellatt et al., 2011). However, the suppression of gonadotropin signaling by Amh in zebrafish might not involve changes of gonadotropin expression in the pituitary and Fshr in the ovary. First, the expression of *fshb*, but not *lhb*, decreased instead of increased in the pituitary of adult *amh* mutant (Zhang et al., 2020), which agrees well with the stimulatory effect of AMH on FSH expression and secretion in mammals (Barbotin et al., 2019; Garrel et al., 2016; Kadokawa, 2020). Second, no significant changes in *fshr* expression were observed in ovarian follicles of different stages in *amh* mutant as compared to controls. Similarly, we did not see any changes of expression in *amh* mutant ovary for *cyp19a1a* (ovarian aromatase) and *inhbaa* (activin βA), which are two potential downstream genes for follicle activation (Fig. S5). Therefore, the suppression of Fshr signaling by Amh may likely take place at the post-receptor level. This will be an interesting issue to explore in future studies. The inhibition of gonadotropin signaling by AMH/Amh at the gonadal level in both mammals and fish suggests a conserved local mechanism that keeps gonadotropin action in check to maintain gonadal homeostasis. The loss of Amh in the gonads would remove such inhibition, therefore intensifying gonadotropin signaling, which in turn induces hyper-proliferation of germ cells.

What is puzzling then is why an enhanced gonadotropin signaling in *amh* mutant was associated with reduced germ cell differentiation, viz. meiosis in the testis and PG-PV transition in the ovary. Our hypothesis is that while Amh suppresses gonadotropin-stimulated germ cell proliferation, it plays a permissive role to gonadotropin-stimulated germ cell differentiation, viz. meiosis in testis and follicle activation in ovary. This idea is supported by our evidence that without *fshr* (-/- female) or *fshr/lhcgr* (-/-;-/- male), the PG-PV transition in the ovary and meiosis in the testis stopped completely regardless of presence or absence of Amh (+/- or -/-), suggesting that Amh itself is not sufficient to drive germ cell differentiation. These activities resumed, but only to a very limited extent, in the presence of *fshr* (+/- female) or *fshr/lhcgr* (+/-;+/- male) but absence of *amh* (-/-). Full scale differentiation (meiosis and PG-PV transition) occurred in the presence of all genes ($amh^{+/-};fshr^{+/-}$ in female and $amh^{+/-};fshr^{+/-};lhcgr^{+/-}$ in male). The dual roles played by Amh in modulating gonadotropin signaling (inhibitory for germ cell proliferation but stimulatory for differentiation) makes Amh a critical gonadal factor in maintaining gonadal homeostasis and normal gametogenesis.

Evidence for Bmpr2a-mediated Amh signaling in zebrafish

As a member of transforming growth factor-β (TGF-β) superfamily, AMH is well known for its signaling through a specific type II receptor AMHRII (Mishina et al., 1996). Knockout of AMHRII in mice showed that the male mutant developed both male and female reproductive tract systems including uterus and oviduct, fully phenocopying AMH ligand mutant (Mishina et al., 1996). In teleosts, a previous study in medaka characterized a mutant (*hotei*) that showed enormous gonadal sizes, and the mutant gene was identified as Amh type II receptor *amhr2* (Morinaga et al., 2007). Similar phenotypes have also been reported in *amh* mutants of zebrafish (Lin et al., 2017; Yan et al., 2019; Zhang et al., 2020) and *amh*/*amhr2* mutants in tilapia (Liu et al., 2019), suggesting Amh-Amhr2 signaling in teleosts. However, what is intriguing is that no homolog of *amhr2* has been found in the zebrafish genome. How would Amh signal in zebrafish then? Our hypothesis is that without its cognate type II receptor, Amh may bind and signal through a closely related receptor in the TGF-β family. Phylogenetic analysis showed that BMP type II receptors (*bmpr2a/bmpr2b*) have the closest genetic relation with Amhr2 cluster among all the type II receptors of TGF-β family ligands.

To test this hypothesis, we generated two mutant zebrafish lines for *bmpr2a* and *bmpr2b* respectively. Phenotype analysis demonstrated distinct functions for *bmpr2a* and *bmpr2b* in zebrafish, suggesting neo-functionalization and/or sub-functionalization for these genes after genome duplication. Unexpectedly, neither *bmpr2a* nor *bmpr2b* single mutants exhibited any developmental defects despite the well-known importance of BMP family in embryogenesis and organogenesis (Chen et al., 2004); however, double mutant of *bmpr2a* and *bmpr2b* (*bmpr2a*$^{-/-}$;*bmpr2b*$^{-/-}$) exhibited severe juvenile mortality with significant developmental defects after 15 dpf, suggesting functional complementation of Bmpr2a and Bmpr2b in zebrafish embryonic and larval development. By comparison, BMPRII null mice died much earlier at embryonic stage (Beppu et al., 2000).

Despite the lack of phenotypes of Bmpr2a and Bmpr2b single mutants in development and growth, they both exhibited unique phenotypes in reproduction. Surprisingly, the loss of *bmpr2a* fully phenocopied those of *amh* mutant in both males and females. The female mutant (*bmpr2a*$^{-/-}$) exhibited abnormal folliculogenesis with accumulation of PG follicles and gradual depletion of advanced follicles, and male

mutant had enormous testis with abundant spermatogonia. These phenotypes were identical to those of *amh* mutant in zebrafish (Lin et al., 2017; Yan et al., 2019; Zhang et al., 2020) and tilapia (Liu et al., 2019), as well as *amhr2* mutant in medaka (Morinaga et al., 2007) and tilapia (Liu et al., 2019). In addition, both *amh* and *bmpr2a* mutants had significantly reduced *fshb* expression in the pituitary (Zhang et al., 2020). These results strongly suggest a potential role for *bmpr2a* to function as the Amh type II receptor (Amhr2) in zebrafish, therefore filling up a missing link in this species. In support of this idea is that double mutant of *amh* and *bmpr2a* (*amh*$^{-/-}$;*bmpr2a*$^{-/-}$) showed no additive phenotypic effects as compared to the single mutants of *amh* and *bmpr2a*, and the three genotypes showed no significant phenotypic difference in terms of both GSI and histological morphology (*amh*$^{-/-}$;*bmpr2a*$^{+/-}$, *amh*$^{+/-}$;*bmpr2a*$^{-/-}$, and *amh*$^{-/-}$;*bmpr2a*$^{-/-}$), further suggesting that they are working in the same signaling pathway. This agrees well with the study in mice in which double mutant of AMH and AMHRII showed indistinguishable phenotypes from those of single mutants (Mishina et al., 1996). The adoption of Bmpr2a as Amhr2 to mediate Amh signaling in zebrafish is not surprising because TGF-β family members often show high degree of ligand-receptor promiscuity (Santibanez et al., 2011) and both BMP and AMH are known to suppress follicle sensitivity to FSH in mammals (Visser and Themmen, 2014). In zebrafish, our previous study showed that recombinant zebrafish BMP2b and BMP4 significantly suppressed *fshr* but stimulated *lhcgr* expression in cultured follicle cells (Li et al., 2012).

Interestingly, a mutation in a putative BMP type I receptor, *bmpr1bb/alk6b*, also caused similar gonadal defects in zebrafish (Neumann et al., 2011). Based on this and our results, we propose that as a gonad-specific growth factor, Amh may act through the signaling cascade of Amh-Bmpr2a-Bmpr1bb to control gonadal development in zebrafish (Fig. 7).

Distinct roles of Bmpr2b in folliculogenesis

Our previous study reported spatiotemporal expression profiles of BMP ligands (*bmp2a*, *bmp2b*, *bmp4*, *bmp6*, and *bmp7a*) and BMP type II receptors (*bmpr2a* and *bmpr2b*) in zebrafish follicles. The ligands examined were expressed primarily in the oocyte, whereas their type II receptors *bmpr2a* and *bmpr2b* were exclusively localized in the surrounding follicle cells, suggesting a BMP-mediated paracrine regulation between the oocyte and somatic follicle cells. The two receptors *bmpr2a* and *bmpr2b*

showed increased expression during folliculogenesis, with the highest levels reached at the FG stage (Li and Ge, 2011), suggesting roles for BMP signaling in follicle growth and maturation.

After demonstrating that *bmpr2a* may serve as the receptor for Amh in controlling gonadal development and function, we then turned our attention to *bmpr2b*. The results showed entirely different phenotypes between *bmpr2a* and *bmpr2b* mutants. In contrast to *bmpr2a*, the loss of *bmpr2b* (*bmpr2b*$^{-/-}$) had no effect on males, which showed normal testis development and spermatogenesis. In contrast, the female *bmpr2b* mutant showed severe reproductive defects. The mutant females were infertile because the follicles could only grow to EV or maximally MV stage, not full-sized FG stage, and the ovulated eggs could not be fertilized. This suggests that BMP-Bmpr2b signaling pathway plays an important role in controlling vitellogenic growth in zebrafish.

The distinct phenotypes of *bmpr2a* and *bmpr2b* mutants strongly suggest neo-functionalization of the two receptors after genome duplication. Bmpr2a takes up a new role to serve as Amh type II receptor, therefore filling up the missing link for Amh signaling in zebrafish, which lacks the cognate Amh type II receptor (Amhr2). In contrast, Bmpr2b has nothing to do with Amh signaling and it plays a critical role in folliculogenesis, most likely by mediating the BMP signals from the growing oocytes.

In conclusion, the present study confirmed Amh functions reported in zebrafish and provided critical genetic evidence for its interaction with gonadotropin signaling in the gonads. The key discoveries can be summarized as follows: 1) Amh deficiency induced severe disturbance to gonadal homeostasis and gametogenesis in both males and females; 2) Amh inhibits germ cell proliferation by suppressing gonadotropin action but stimulates germ cell differentiation by promoting gonadotropin signaling; and 3) Amh may signal via Bmpr2a receptor in the absence of its cognate Amhr2 receptor.

Materials and methods

Fish and maintenance

The AB strain zebrafish was used in the present study. The larval fish were first raised in an environmental chamber (Model 3949; Thermo Scientific) with paramecium. They were transferred to the ZebTEC Multilinking Rack Zebrafish System (Tecniplast, Buguggiate, Italy) after starting to feed on brine shrimp (*Artemia*). The system was under the photocycle of 14-h light and 10-h dark with temperature, pH and conductivity being 28±1℃, 7.5 and 400 μS/cm, respectively. All experiments were performed according to the protocols approved by the Research Ethics Committee of University of Macau.

Establishment of mutant lines

Zebrafish mutant lines were established using CRISPR/Cas9 method according to the protocols reported previously (Lau et al., 2016). The online tool ZIFIT Targeter (http://zifit.partners.org/zifit) was used to design CRISPR target sites. The single guide RNAs (sgRNAs) and Cas9 RNA were prepared using MEGAscript T7 and mMESSAGE mMACHINE SP6 kits (Life Technologies, Carlsbad, CA), respectively. About 100 pg sgRNA and 400 pg Cas9 mRNA were co-injected into one or two-cell stage embryos with the Drummond Nanoject system (Drummond Scientific, Broomall, PA). Mutagenesis was first screened at 24 h post fertilization (hpf) using both high resolution melting analysis (HRMA) and heteroduplex mobility assay (HMA) (Zhang et al., 2015a; Zhang et al., 2015b). The F0 adults were genotyped on DNA extracted from the caudal fin for mutagenesis followed by sequence confirmation (Zhang et al., 2015b). The sibling F1 females and males carrying the same frameshift mutation (+/-) were crossed to obtain homozygous F2 (-/-) offspring for phenotype analysis. The primers used for HRMA/HMA are listed in Supplemental Table 1.

Sampling and histological examination

The fish were anaesthetized by MS222 (Sigma, St. Louis, MO) before handling. Each fish was photographed with digital camera (Canon EOS 700D) to record gross morphology before measurement of body weight, standard body length and the gonadosomatic index (GSI, gonad weight/body weight). For histological analysis, the

entire fish or dissected gonads were fixed in Bouin's fixative for 24 h before processing on the ASP6025S Automatic Vacuum Tissue Processor (Leica, Wetzlar, Germany). After paraffin embedding, the samples were serially sectioned at 5 μm, stained with hematoxylin and eosin (H&E), and viewed on Nikon ECLIPSE Ni-U microscope (Nikon, Tokyo, Japan). The images were photographed with the Digit Sight DS-Fi2 digital camera (Nikon).

Fertility and survival test

The fish were crossed with the wild type partners either for individual or group test. The fecundity of the females refers to the number of the ovulated eggs at 0-1 hpf, and the fertility refers to normal fertilization and embryogenesis as well as viability of the offspring. The survival rate was calculated based on the ratios of different genotypes at different time points from 0 to 60 dpf at 15-day intervals.

Fin regeneration

The caudal fins were amputated at 35 dpf (Day 0), and the regeneration process was recorded by photographing at Day 3 and 6, respectively.

RNA extraction and quantitative real-time qPCR

Total RNA was extracted from ovary or testis using TRIzol (Invitrogen, Carlsbad, CA) according to the manufacture's protocol. The extracted RNA was reverse transcribed to cDNA using MMLV reverse transcriptase (Invitrogen, Carlsbad, CA) as previously reported (Zhang et al., 2015a; Zhang et al., 2015b). The primers used for real-time qPCR are listed in Supplemental Table 1. The expression levels of target genes were normalized to that of the housekeeping gene *ef1a*, and expressed as the fold change compared to the control group.

Immunofluorescence

Sections from paraffin-embedded samples were mounted on slides, followed by de-paraffinization in xylene and rehydration with serially diluted ethanol. Antigen retrieval was performed by placing the slides in sub-boiling citrate buffer for 10 min. The sections were washed with PBST buffer 3 times for 5 min each, and then blocked with 10% heat-inactivated horse serum for 1 h at room temperature in a humidified

chamber. The slides were incubated with primary antibody (1:100, anti-pSMAD1/5/8; AB3848-1) (Millipore, Bedford, MA) overnight at 4℃. After washing with PBST buffer 5 times for 5 min each, the slides were incubated with the secondary antibody (1:1000, Alex Fluor 488) (Cell Signaling Technology, Danvers, MA) for 2 h at room temperature. After washing with PBS 5 times for 5 min each, the sections were stained with DAPI (0.5 μg/ml; Roche, Mannheim, Germany) for 5 min. The sections were then mounted with ProLong Gold antifade reagent (Invitrogen, Carlsbad, CA) and sealed with commercial nail oil.

Data analysis

All the values in this study were expressed as mean ± SEM, and statistical significance was analyzed by ANOVA or Student's *t* test using Prism 8 (GraphPad, San Diego, CA). The significant level was indicated as * for $P<0.05$, ** for $P<0.01$, and *** for $P<0.001$.

Acknowledgment

This study was supported by grants from the University of Macau (MYRG2015-00227-FHS, MYRG2016-00072-FHS, MYRG2017-00157-FHS and CPG2014-00014-FHS) and The Macau Fund for Development of Science and Technology (FDCT/089/2014/A2 and FDCT173/2017/A3) to W.G.

References

Barbotin, A. L., Peigne, M., Malone, S. A. and Giacobini, P. (2019). Emerging Roles of Anti-Mullerian Hormone in Hypothalamic-Pituitary Function. *Neuroendocrinology* **109**, 218-229.

Behringer, R. R., Finegold, M. J. and Cate, R. L. (1994). Mullerian-inhibiting substance function during mammalian sexual development. *Cell* **79**, 415-425.

Beppu, H., Kawabata, M., Hamamoto, T., Chytil, A., Minowa, O., Noda, T. and Miyazono, K. (2000). BMP type II receptor is required for gastrulation and early development of mouse embryos. *Dev. Biol.* **221**, 249-258.

Broer, S. L., Broekmans, F. J. M., Laven, J. S. E. and Fauser, B. C. J. M. (2014). Anti-Mullerian hormone: ovarian reserve testing and its potential clinical implications. *Hum. Reprod. Update* **20**, 688-701.

Chen, D., Zhao, M. and Mundy, G. R. (2004). Bone morphogenetic proteins. *Growth Factors* **22**, 233-241.

Durlinger, A. L., Kramer, P., Karels, B., de Jong, F. H., Uilenbroek, J. T., Grootegoed, J. A. and Themmen, A. P. (1999). Control of primordial follicle recruitment by anti-Mullerian hormone in the mouse ovary. *Endocrinology* **140**, 5789-5796.

Durlinger, A. L. L., Gruijters, M. J. G., Kramer, P., Karels, B., Kumar, T. R., Matzuk, M. M., Rose, U. M., de Jong, F. H., Uilenbroek, J. T. J., Grootegoed, J. A., et al. (2001). Anti-Mullerian hormone attenuates the effects of FSH on follicle development in the mouse ovary. *Endocrinology* **142**, 4891-4899.

Durlinger, A. L. L., Visser, J. A. and Themmen, A. P. N. (2002). Regulation of ovarian function: the role of anti-Mullerian hormone. *Reproduction* **124**, 601-609.

Garg, D. and Tal, R. (2016). The role of AMH in the pathophysiology of polycystic ovarian syndrome. *Reprod. Biomed. Online* **33**, 15-28.

Garrel, G., Racine, C., L'Hote, D., Denoyelle, C., Guigon, C. J., di Clemente, N. and Cohen-Tannoudji, J. (2016). Anti-Mullerian hormone: a new actor of sexual dimorphism in pituitary gonadotrope activity before puberty. *Sci. Rep.* **6**, 23790.

Grossman, M. P., Nakajima, S. T., Fallat, M. E. and Siow, Y. (2008). Mullerian-inhibiting substance inhibits cytochrome P450 aromatase activity in human granulosa lutein cell culture. *Fertil. Steril.* **89**, 1364-1370.

Josso, N., Belville, C., di Clemente, N. and Picard, J. Y. (2005). AMH and AMH receptor defects in persistent Mullerian duct syndrome. *Hum. Reprod. Update* **11**, 351-356.

Josso, N. and di Clemente, N. (1999). TGF-β family members and gonadal development. *Trends Endocrinol. Metab.* **10**, 216-222.

Kadokawa, H. (2020). Discovery of new receptors regulating LH and FSH secretion by bovine gonadotrophs to explore a new paradigm for mechanisms regulating reproduction. *Journal of Reproduction and Development* **advpub**.

Kluver, N., Pfennig, F., Pala, I., Storch, K., Schlieder, M., Froschauer, A., Gutzeit, H. O. and Schartl, M. (2007). Differential expression of anti-Mullerian hormone (*amh*) and anti-Mullerian hormone receptor type II (*amhrII*) in the teleost medaka. *Dev. Dyn.* **236**, 271-281.

Lau, E. S., Zhang, Z., Qin, M. and Ge, W. (2016). Knockout of zebrafish ovarian aromatase gene (*cyp19a1a*) by TALEN and CRISPR/Cas9 leads to all-male offspring due to failed ovarian differentiation. *Sci. Rep.* **6**, 37357.

Li, C. W. and Ge, W. (2011). Spatiotemporal expression of bone morphogenetic protein family ligands and receptors in the zebrafish ovary: a potential paracrine-signaling mechanism for oocyte-follicle cell communication. *Biol. Reprod.* **85**, 977-986.

Li, C. W., Zhou, R. and Ge, W. (2012). Differential regulation of gonadotropin receptors by bone morphogenetic proteins in the zebrafish ovary. *Gen Comp Endocrinol* **176**, 420-425.

Lin, Q., Mei, J., Li, Z., Zhang, X., Zhou, L. and Gui, J. F. (2017). Distinct and cooperative roles of *amh* and *dmrt1* in self-renewal and differentiation of male germ cells in zebrafish. *Genetics* **207**, 1007-1022.

Liu, X., Xiao, H., Jie, M., Dai, S., Wu, X., Li, M. and Wang, D. (2019). Amh regulate female folliculogenesis and fertility in a dose-dependent manner through Amhr2 in Nile tilapia. *Mol. Cell. Endocrinol.* **499**, 110593.

Mishina, Y., Rey, R., Finegold, M. J., Matzuk, M. M., Josso, N., Cate, R. L. and Behringer, R. R. (1996). Genetic analysis of the Mullerian-inhibiting substance signal transduction pathway in mammalian sexual differentiation. *Genes Dev.* **10**, 2577-2587.

Monniaux, D., Clement, F., Dalbies-Tran, R., Estienne, A., Fabre, S., Mansanet, C. and Monget, P. (2014). The ovarian reserve of primordial follicles and the dynamic reserve of antral growing follicles: what is the link? *Biol. Reprod.* **90**, 85.

Morinaga, C., Saito, D., Nakamura, S., Sasaki, T., Asakawa, S., Shimizu, N., Mitani, H., Furutani-Seiki, M., Tanaka, M. and Kondoh, H. (2007). The *hotei* mutation of medaka in the anti-Mullerian hormone receptor causes the dysregulation of germ cell and sexual development. *Proc. Natl. Acad. Sci. U. S. A.* **104**, 9691-9696.

Nakamura, S., Watakabe, I., Nishimura, T., Picard, J. Y., Toyoda, A., Taniguchi, Y., di Clemente, N. and Tanaka, M. (2012). Hyperproliferation of mitotically active germ cells due to defective anti-Mullerian hormone signaling mediates sex reversal in medaka. *Development* **139**, 2283-2287.

Neumann, J. C., Chandler, G. L., Damoulis, V. A., Fustino, N. J., Lillard, K., Looijenga, L., Margraf, L., Rakheja, D. and Amatruda, J. F. (2011). Mutation in the type IB bone morphogenetic protein receptor Alk6b impairs germ-cell differentiation and causes germ-cell tumors in zebrafish. *Proc Natl Acad Sci USA* **108**, 13153-13158.

Pellatt, L., Rice, S., Dilaver, N., Heshri, A., Galea, R., Brincat, M., Brown, K., Simpson, E. R. and Mason, H. D. (2011). Anti-Mullerian hormone reduces follicle sensitivity to follicle-stimulating hormone in human granulosa cells. *Fertil. Steril.* **96**, 1246-1251 e1241.

Pfennig, F., Standke, A. and Gutzeit, H. O. (2015). The role of Amh signaling in teleost fish--Multiple functions not restricted to the gonads. *Gen. Comp. Endocrinol.* **223**, 87-107.

Pigny, P., Merlen, E., Robert, Y., Cortet-Rudelli, C., Decanter, C., Jonard, S. and Dewailly, D. (2003). Elevated serum level of anti-mullerian hormone in patients with polycystic ovary syndrome: relationship to the ovarian follicle excess and to the follicular arrest. *J. Clin. Endocrinol. Metab.* **88**, 5957-5962.

Rehman, Z. U., Worku, T., Davis, J. S., Talpur, H. S., Bhattarai, D., Kadariya, I., Hua, G., Cao, J., Dad, R., Farmanullah, et al. (2017). Role and mechanism of AMH in the regulation of Sertoli cells in mice. *J. Steroid Biochem. Mol. Biol.* **174**, 133-140.

Santibanez, J. F., Quintanilla, M. and Bernabeu, C. (2011). TGF-β/TGF-β receptor system and its role in physiological and pathological conditions. *Clin. Sci. (Lond.)* **121**, 233-251.

So, W. K., Kwok, H. F. and Ge, W. (2005). Zebrafish gonadotropins and their receptors: II. Cloning and characterization of zebrafish follicle-stimulating hormone and luteinizing hormone subunits - their spatial-temporal expression patterns and receptor specificity. *Biol. Reprod.* **72**, 1382-1396.

Vigier, B., Picard, J. Y., Tran, D., Legeai, L. and Josso, N. (1984). Production of anti-Mullerian hormone: another homology between Sertoli and granulosa cells. *Endocrinology* **114**, 1315-1320.

Visser, J. A., Durlinger, A. L. L., Peters, I. J. J., van den Heuvel, E. R., Rose, U. M., Kramer, P., de Jong, F. H. and Themmen, A. P. N. (2007). Increased oocyte degeneration and follicular atresia during the estrous cycle in anti-Mullerian hormone null mice. *Endocrinology* **148**, 2301-2308.

Visser, J. A., Schipper, I., Laven, J. S. and Themmen, A. P. (2012). Anti-Mullerian hormone: an ovarian reserve marker in primary ovarian insufficiency. *Nat. Rev. Endocrinol.* **8**, 331-341.

Visser, J. A. and Themmen, A. P. (2005). Anti-Mullerian hormone and folliculogenesis. *Mol. Cell. Endocrinol.* **234**, 81-86.

Visser, J. A. and Themmen, A. P. N. (2014). Role of anti-Mullerian hormone and bone morphogenetic proteins in the regulation of FSH sensitivity. *Mol. Cell. Endocrinol.* **382**, 460-465.

Yan, Y. L., Batzel, P., Titus, T., Sydes, J., Desvignes, T., BreMiller, R., Draper, B. and Postlethwait, J. H. (2019). A hormone that lost its receptor: anti-Müllerian hormone (AMH) in zebrafish gonad development and sex determination. *Genetics* **213**, 529-553.

Zhang, Z., Lau, S. W., Zhang, L. and Ge, W. (2015a). Disruption of zebrafish follicle-stimulating hormone receptor (*fshr*) but not luteinizing hormone receptor (*lhcgr*) gene by TALEN leads to failed follicle activation in females followed by sexual reversal to males. *Endocrinology* **156**, 3747-3762.

Zhang, Z., Zhu, B., Chen, W. and Ge, W. (2020). Anti-Mülllerian hormone (Amh/amh) plays dual roles in maintaining gonadal homeostasis and gametogenesis in zebrafish. *Mol. Cell. Endocrinol.*, 110963.

Zhang, Z., Zhu, B. and Ge, W. (2015b). Genetic analysis of zebrafish gonadotropin (FSH and LH) functions by TALEN-mediated gene disruption. *Mol. Endocrinol.* **29**, 76-98.

Zhou, R., Tsang, A. H., Lau, S. W. and Ge, W. (2011). Pituitary adenylate cyclase-activating polypeptide (PACAP) and its receptors in the zebrafish ovary: evidence for potentially dual roles of PACAP in controlling final oocyte maturation. *Biol. Reprod.* **85**, 615-625.

Figures

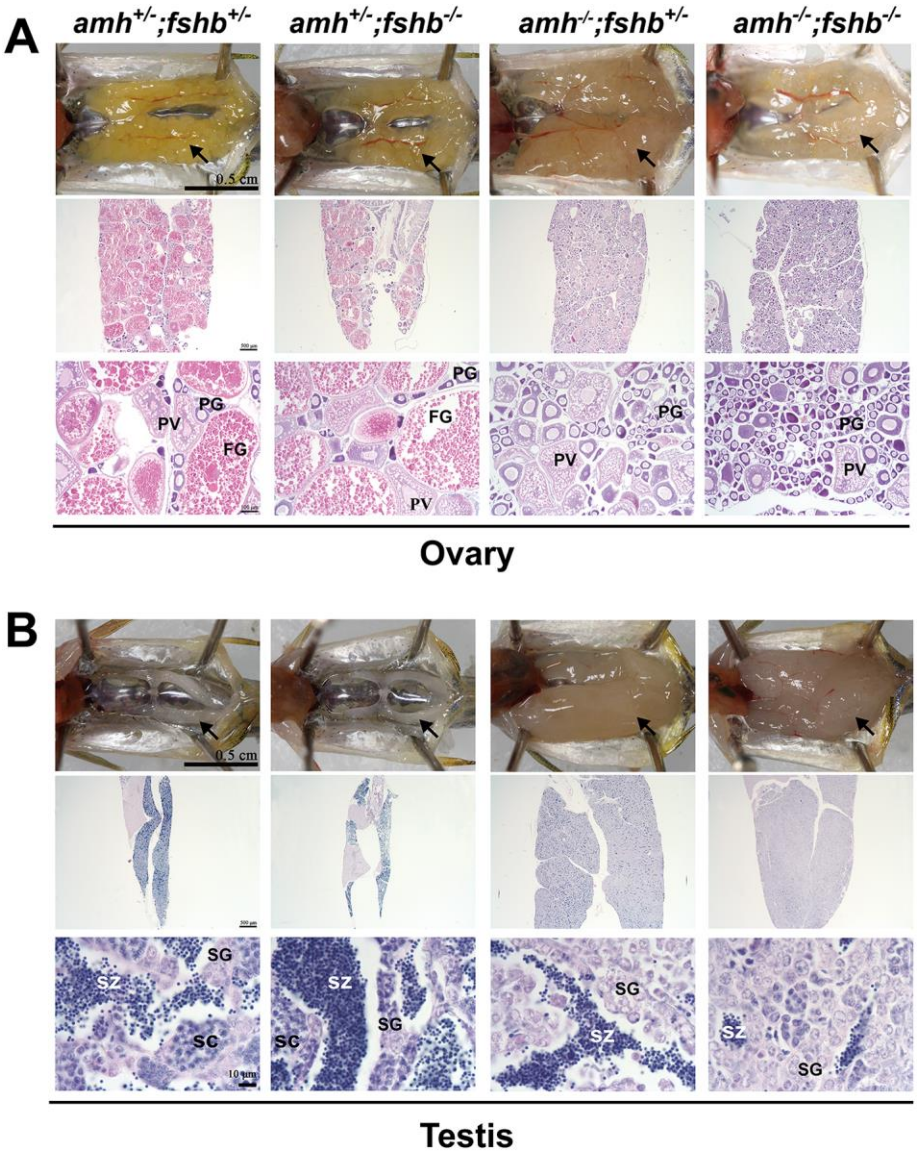

Fig. 1. Gonadal histology of *amh* mutant and double mutant with *fshb* mutation at 4 mpf. (A) Ovaries of four different genotypes: control *($amh^{+/-};fshb^{+/-}$)*, *fshb* single mutant *($amh^{+/-};fshb^{-/-}$)*, *amh* single mutant *($amh^{-/-};fshb^{+/-}$)*, and *amh* and *fshb* double mutant *($amh^{-/-};fshb^{-/-}$)*. (B) Testes of four different genotypes. PG: primary growth; PV: pre-vitellogenic; FG: full-grown; SG: spermatogonia; SC: spermatocytes; SZ: spermatozoa; arrows: ovaries and testes.

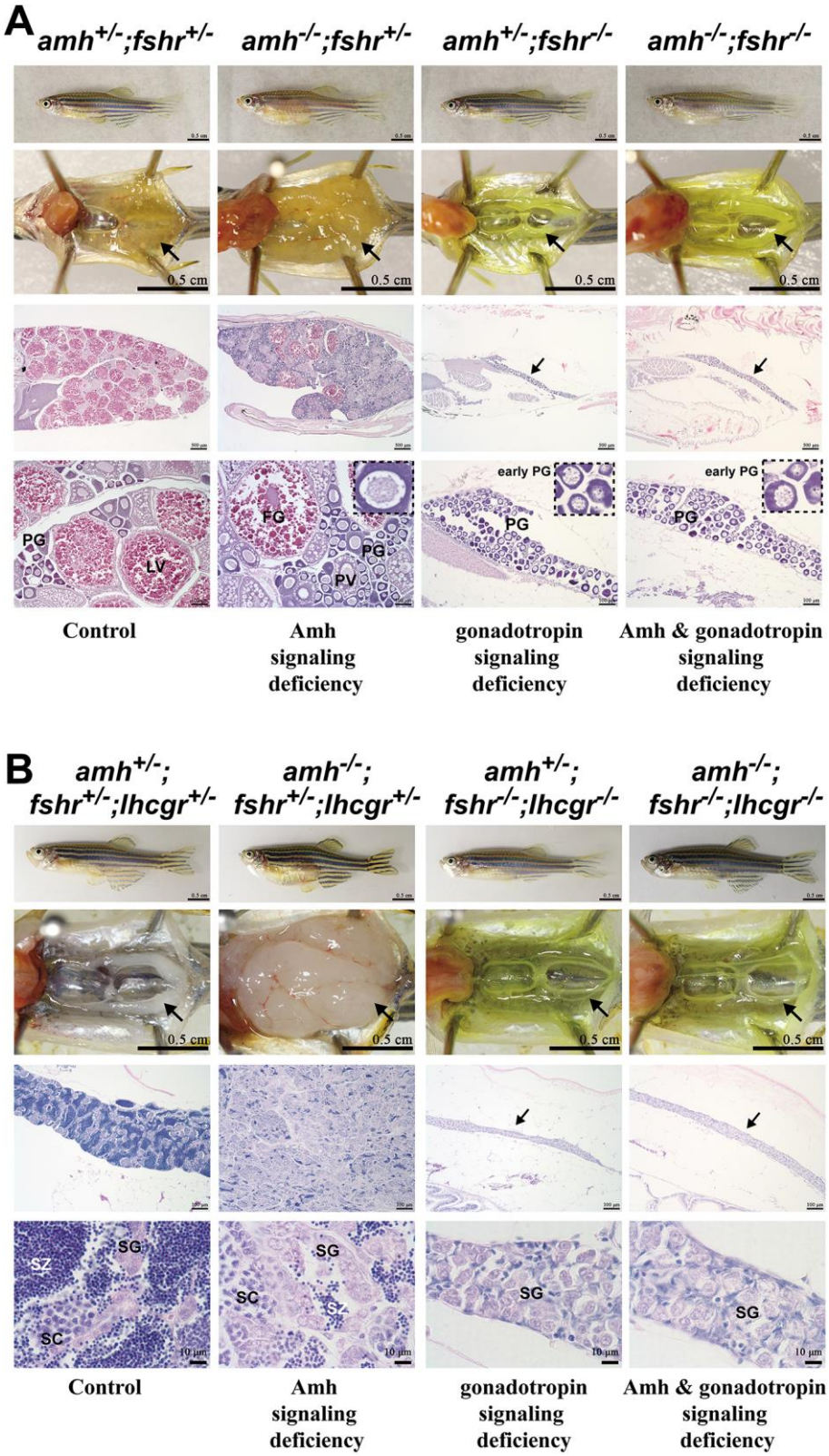

Fig. 2. Evidence for involvement of gonadotropin signaling in *amh* deficiency-induced gonadal hypergrowth and dysfunctional gametogenesis. (A) Ovaries of different

genotypes at 5 mpf. While *amh* single mutation (*amh*$^{-/-}$;*fshr*$^{+/-}$) caused ovarian hypertrophy with accumulation of PG follicles, the *fshr* single mutant (*amh*$^{+/-}$;*fshr*$^{-/-}$) showed ovarian hypotrophy with much less and underdeveloped PG follicles only. Double mutation of *amh* and *fshr* (*amh*$^{-/-}$;*fshr*$^{-/-}$) completely abolished the phenotype of *amh* mutant. (B) Testes of different genotypes at 5 mpf. Amh mutation alone (*amh*$^{-/-}$;*fshr*$^{+/-}$;*lhcgr*$^{+/-}$) caused testis hypertrophy and dysfunctional spermatogenesis with limited meiosis, whereas the loss of gonadotropin signaling in *fshr* and *lhcgr* double mutant (*amh*$^{+/-}$;*fshr*$^{-/-}$;*lhcgr*$^{-/-}$) led to testis hypotrophy and dysfunctional spermatogenesis with no meiosis. The loss of all the three genes in the triple knockout (*amh*$^{-/-}$;*fshr*$^{-/-}$;*lhcgr*$^{-/-}$) completely abolished the hypertrophic phenotype of *amh* mutation. arrows: hypotrophic ovaries and testes. PG: primary growth; PV: pre-vitellogenic; LV: late vitellogenic; FG: full-grown; SG: spermatogonia; SC: spermatocytes; SZ: spermatozoa; arrows: ovaries and testes.

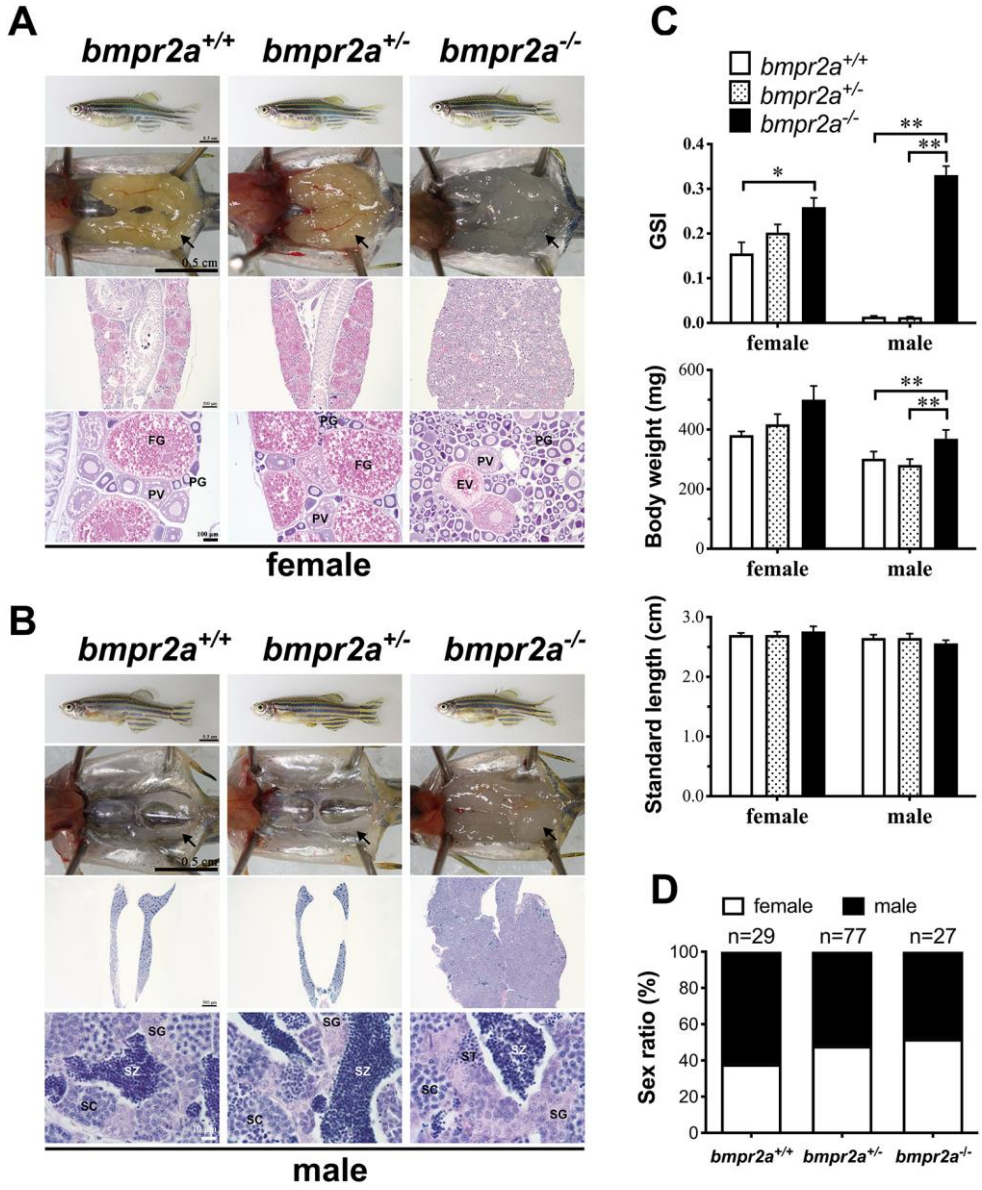

Fig. 3. Gonadal hypertrophy in *bmpr2a* mutant. (A) Ovaries of different genotypes at 5 mpf. Bmpr2a mutation (*bmpr2a*$^{-/-}$) caused significant enlargement of the ovary containing large number of PG follicles with only a few entering PV and vitellogenic growth. (B) Testes of different genotypes at 5 mpf. Bmpr2a mutation also induced hypertrophic growth of the testis, which contained abundant spermatogonia with limited meiosis. (C) Body length, body weight and gonadosomatic index (GSI) of different genotypes (n=5; * $P < 0.05$, ** $P < 0.01$). (D) Sex ratios in different genotypes. PG: primary growth; PV: pre-vitellogenic; EV: early vitellogenic; FG: full-grown; SG: spermatogonia; SC: spermatocytes; ST: spermatids; SZ: spermatozoa; arrows: ovaries and testes.

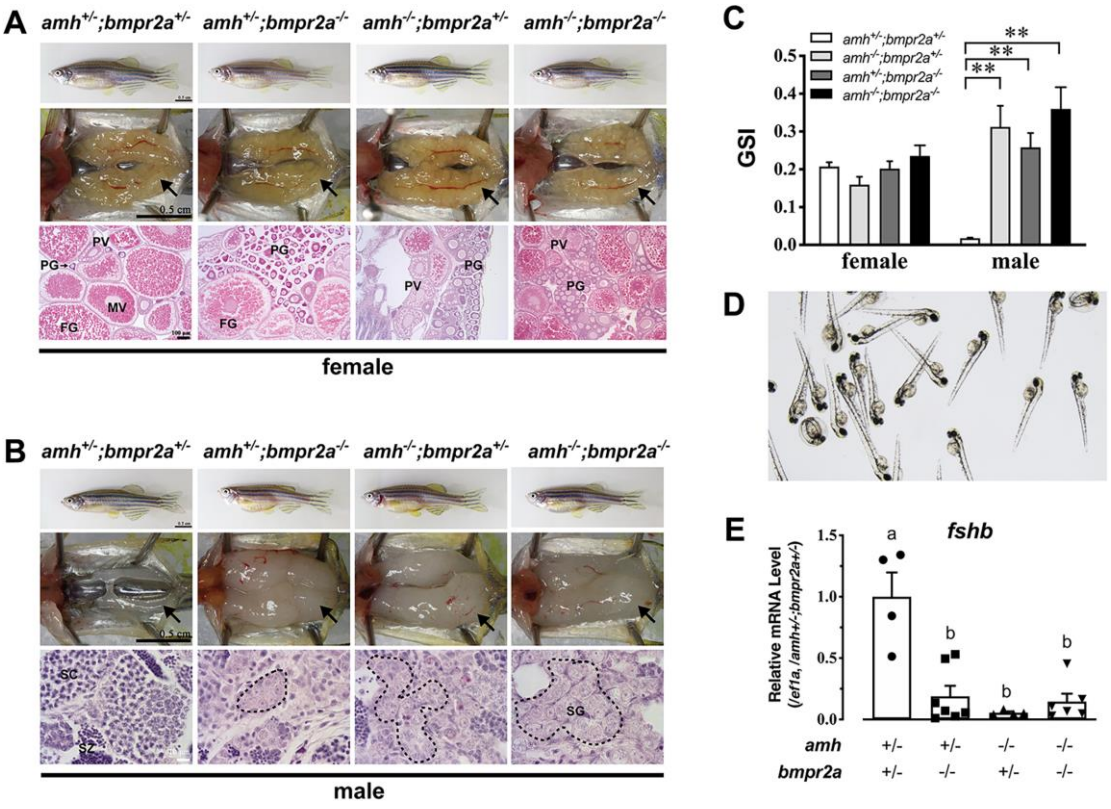

Fig. 4. Phenotype analysis of *amh* and *bmpr2a* double mutant at 3 mpf. (A) Ovaries of different genotypes. There was a significant accumulation of PG follicles in *amh* single mutant (*amh*$^{-/-}$;*bmpr2a*$^{+/-}$), *bmpr2a* single mutant (*amh*$^{-/-}$;*bmpr2a*$^{-/-}$), and *amh* and *bmpr2a* double mutant (*amh*$^{-/-}$;*bmpr2a*$^{-/-}$) as compared to the control (*amh*$^{+/-}$;*bmpr2a*$^{+/-}$). (B) Testes of different genotypes at 3 mpf. All three mutants (*amh* and *bmpr2a* single and double mutants) displayed tremendous testicular hypertrophy with abundant spermatogonia (circled with dotted lines) without any additive effect. (C) GSI of different genotypes (n=5; ** $P < 0.01$). (D) Viable offspring (3 pdf) from male and female double mutants (*amh*$^{-/-}$;*bmpr2a*$^{-/-}$). (E) Expression of *fshb* in the pituitary of *amh* and *bmpr2a* single and double mutants. Different letters indicate statistical significance [n = 4 (*amh*$^{+/-}$;*bmpr2a*$^{+/-}$), 7 (*amh*$^{+/-}$;*bmpr2a*$^{-/-}$), 4 (*amh*$^{-/-}$;*bmpr2a*$^{+/-}$) and 6 (*amh*$^{-/-}$;*bmpr2a*$^{-/-}$)].

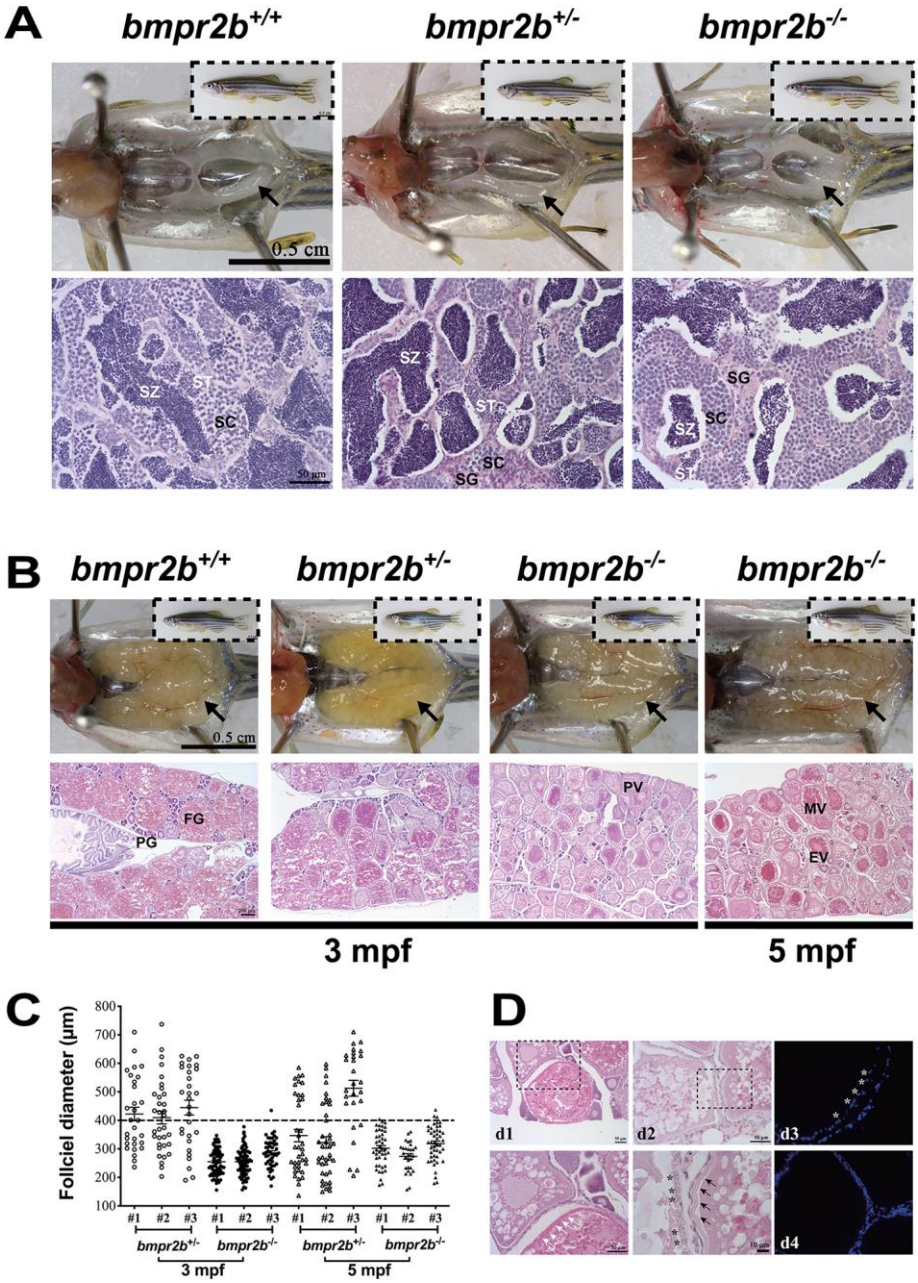

Fig. 5. Phenotype analysis of *bmpr2b* mutant. (A) Normal testis growth and spermatogenesis in male *bmpr2b* mutant at 3 mpf. (B) Ovarian defects in female *bmpr2b* mutant at 3 and 5 mpf. Folliculogenesis was arrested at MV stage in *bmpr2b* mutant at both 3 and 5 mpf. (C) Follicle diameters measured on histological section. Two distant sections from each individual were chosen for quantification of PV and vitellogenic follicles with germinal vesicle visible, and three individuals of each genotype (#1-#3) were analyzed at 3 and 5 mpf. (D) Follicle atresia in the ovary of *bmpr2b* mutants showing abnormal chorion

(arrows in d1 and d2) and hypertrophic granulosa cells (asterisks in d2). DAPI staining showed the hypertrophic granulosa cells (asterisks in d3) as compared to normal follicles (d4). PG: primary growth; PV: pre-vitellogenic; EV: early vitellogenic; MV: mid-vitellogenic; FG: full-grown; SG: spermatogonia; SC: spermatocytes; ST: spermatids; SZ: spermatozoa; arrows: ovaries and testes.

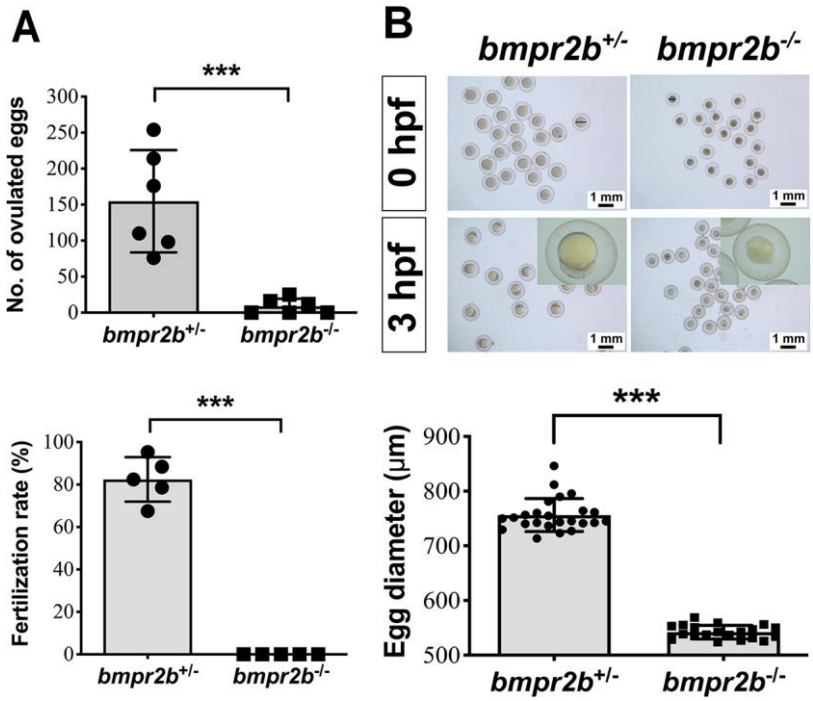

Fig. 6. Fertility test of *bmpr2b* mutant. The mutant (*bmpr2b*$^{-/-}$) and control females (*bmpr2b*$^{+/-}$) were crossed with the wild type male partners. (A) The number of ovulated eggs (0 hpf) and fertilization rate (3 hpf). (B) Diameters of the eggs released. *** $P < 0.001$.

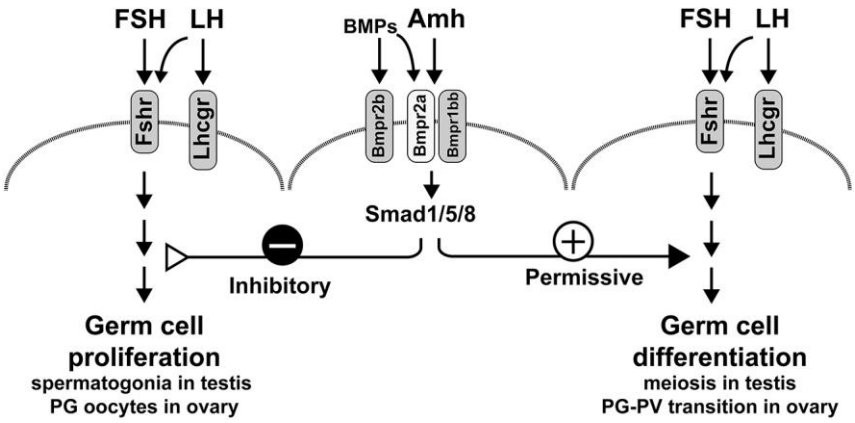

Fig. 7. Hypothetical model for interactions of Amh and gonadotropin signaling pathway in zebrafish gonads. Unlike other species, zebrafish lacks Amh cognate type II receptor (Amhr2). Instead, Amh in zebrafish may likely signal through a closely related BMP type II receptor, Bmpr2a, which then recruits Bmpr1bb/Alk6b as its type I receptor for activating the canonical Smad1/5/8 pathway. Mutations of *amh*, *bmpr2a* and *bmpr1bb* in zebrafish produced identical phenotypes in gonads, viz. gonadal hypertrophy with increased proliferation of germ cells (spermatogonia in the testis and PG follicles in the ovary) and decreased differentiation or exit of germ cells to advanced stages (meiosis in the testis and PG-PV transition in the ovary). Amh in the gonads plays a negative role of inhibiting germ cell proliferation by suppressing gonadotropin signaling while playing a positive role of promoting germ cell differentiation (meiotic division in the testis and follicle activation or PG-PV transition in the ovary) by being permissive to gonadotropin signaling. By controlling both germ cell proliferation and their exit for maturation, Amh serves as a critical local factor in maintaining gonadal homeostasis for steady production of mature gametes in both sexes.

Supplemental Figures and Tables

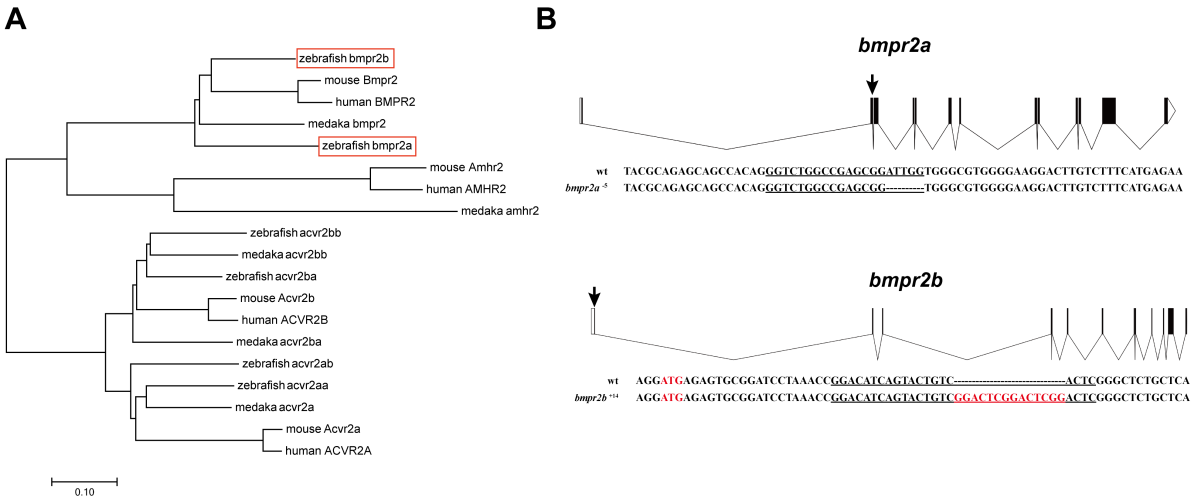

Fig. S1. Bmpr2 receptors (*bmpr2a* and *bmpr2b*) in zebrafish

(A) Phylogenetic analysis of zebrafish *bmpr2a* and *bmpr2b*. The sequences were obtained from Genbank and Ensemble databases. Sequence alignment and tree construction were performed by MEGA software using Neighbor-Joining method. (B) Schematic illustration of CRISPR targeting sites of *bmpr2a* and *bmpr2b* in zebrafish. The arrows indicate the location of targeting sites. Open and solid boxes indicate untranslated and coding exons respectively. Sequences underlined indicate the CRISPR targeting sites and the underlined sequences in red are inserted bases.

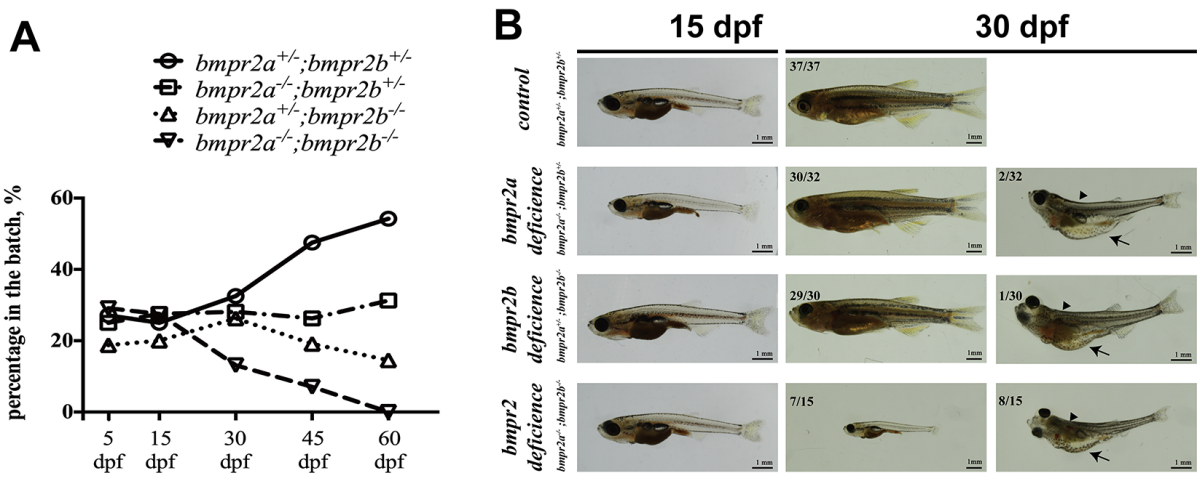

Fig. S1 Bmpr2 deficiency leads to severe developmental defects

The female *bmp2a*$^{-/-}$;*bmpr2b*$^{+/-}$ was crossed with male *bmp2a*$^{+/-}$;*bmpr2b*$^{-/-}$ to produce the offspring with theoretical ratios 1:1:1:1 for different genotypes. The offspring were sampled at different time points (5-60 dpf) for genotyping (A). No obvious abnormalities were observed before 15 dpf among the four genotypes: wild type control (*bmp2a*$^{+/-}$;*bmpr2b*$^{+/-}$), single mutants (*bmp2a*$^{-/-}$;*bmpr2b*$^{+/-}$ and *bmpr2b*$^{+/-}$;*bmpr2b*$^{-/-}$) and double mutant (*bmp2a*$^{-/-}$;*bmpr2b*$^{-/-}$) in terms of survival rate, morphology and growth. However, a significant mortality was observed in the *bmpr2*-deficient double mutant at 30 dpf. The double mutant individuals (*bmp2a*$^{-/-}$;*bmpr2b*$^{-/-}$) that survived at this age all showed obvious developmental defects including edematous abdominal cavity (8 out of 15) and retarded body growth with much smaller body size (7/15) (B). From 30 to 60 dpf, the ratio of double mutant continued to decrease progressively; however, the ratios of the wild type and single mutants did not increase proportionally with the wild type steadily increasing while the single mutants remaining relative constant.

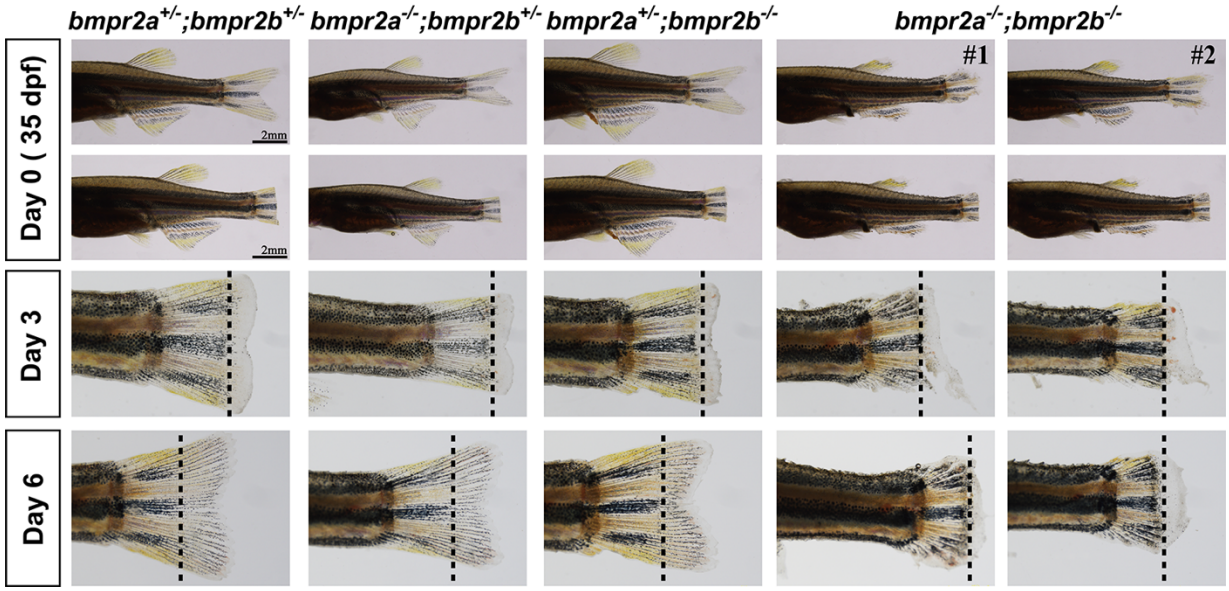

Fig. S2 Defective fin regeneration due to *bmpr2* deficiency

In addition to abdominal edema and retarded growth, some survived double mutants showed abnormal morphology of caudal fin at 35 dpf. To further confirm the role of *bmpr2* signaling in fin development, we performed a caudal fin regeneration assay by amputating the caudal fins at 35 dpf. The dotted line indicates the initial amputation plane. The double mutants (*bmpr2a*$^{-/-}$;*bmpr2b*$^{-/-}$) displayed a quick regeneration with epidermal outgrowth beyond the amputation plane, similar to the single mutants (*bmpr2a*$^{-/-}$;*bmpr2b*$^{+/-}$ and (*bmpr2a*$^{+/-}$;*bmprb2*$^{-/-}$) and control (*bmpr2a*$^{+/-}$;*bmpr2b*$^{+/-}$) at 3 days post amputation (dpa). At 6 dpa, the control and single mutants had fully regenerated the caudal fins with fin rays well developed and tail fork well formed; in contrast, the regeneration of the caudal fins in the double mutants remained unchanged as compared to that at 3 dpa and the regenerated region was covered by the epidermis only without fin rays. The data suggested that *bmpr2* signaling was essential for maintaining normal fin morphology and promoting fin regeneration, and that Bmpr2a and Bmpr2b could functionally compensate for each other in this regard.

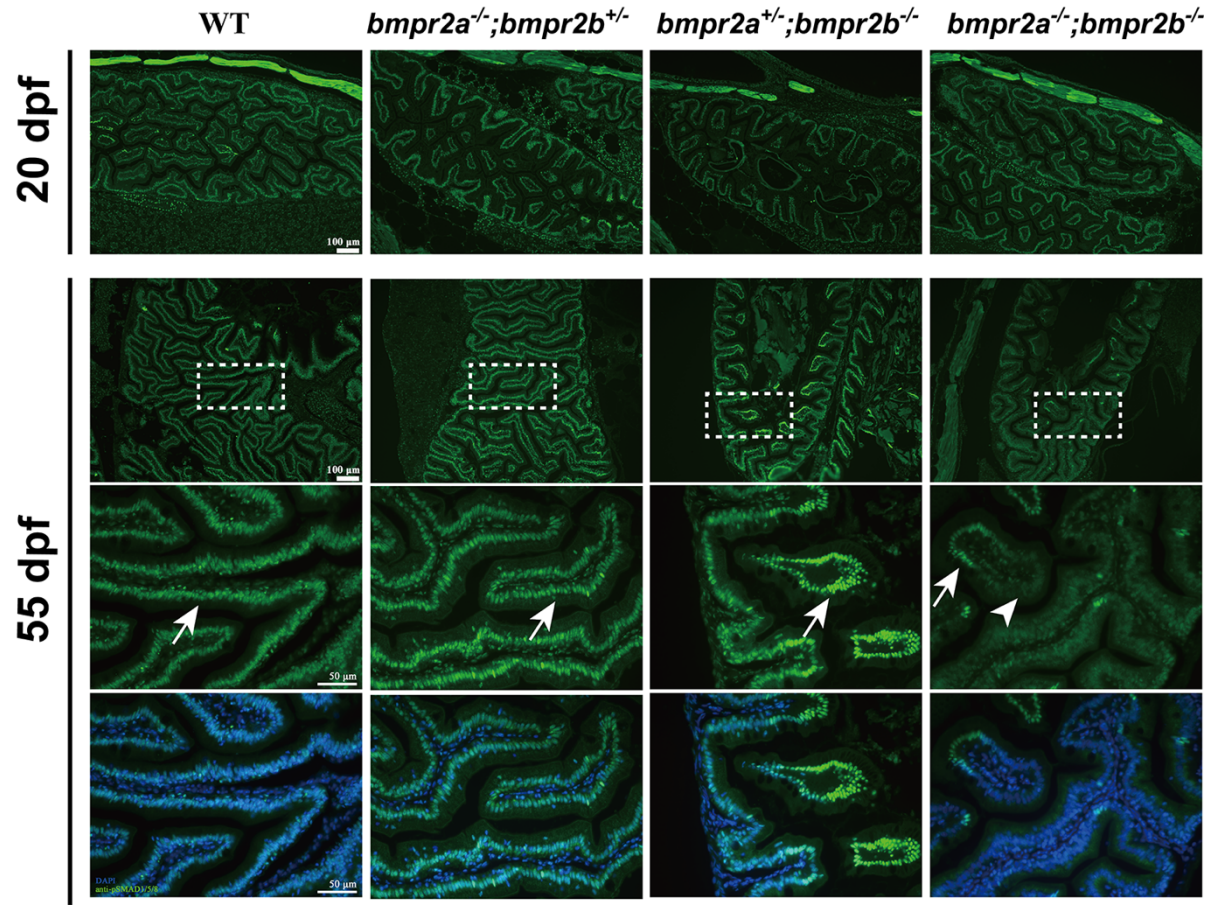

Fig. S3 Bmpr2 deficiency reduces Smad1/5/8 phosphorylation in the intestine

To demonstrate whether the *bmpr2a* and/or *bmpr2b* mutation disrupts BMP signaling activity, we examined the phosphorylation of Smad1/5/8 by immunofluorescent staining for the signal of phosphor-Smad1/5/8 (pSmad1/5/8). At 20 dpf, a strong pSmad1/5/8 signal was observed in the intestines of all genotypes including control (WT), *bmpr2a* and *bmpr2b* single mutants (*bmpr2a*$^{-/-}$;*bmpr2b*$^{+/-}$ and *bmpr2a*$^{+/-}$;*bmpr2b*$^{-/-}$), and the *bmpr2a*-deficient double mutant (*bmpr2a*$^{-/-}$;*bmpr2b*$^{-/-}$). At 55 dpf, the pSmad1/5/8 signal remained strong in the intestinal epithelial cells in control and single mutants (arrows); however, the signal was absent in most of the epithelium cells of the *bmpr2*-deficient double mutants (arrowhead). Interestingly, this was the time window when most double mutants died.

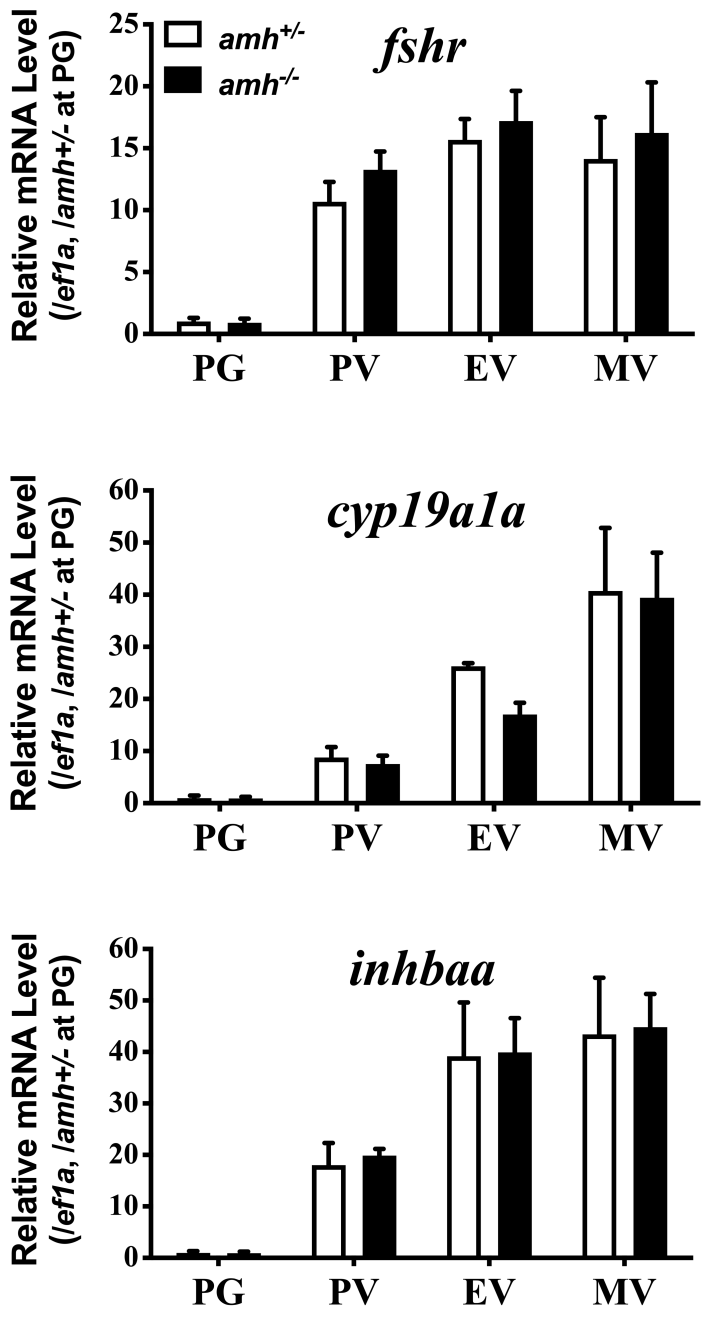

Fig. S4 Expression of *fshr* (FSH receptor), *cyp19a1a* (ovarian aromatase) and *inhbaa* (activin βA) in follicles of *amh* mutant

Follicles of PG (primary growth), PV (pre-vitellogenic), EV (early vitellogenic) and MV (mid-vitellogenic) were isolated from *amh* mutant ($amh^{-/-}$) and control fish ($amh^{+/-}$) for RNA extraction and qPCR quantification. The expression level of each target gene was normalized to the housekeeping gene *ef1a* in the same sample and expressed as the ratio to that of control PG ($amh^{+/-}$). The values are mean ± SEM (n = 3). No significant difference was observed between *amh* mutant and control at any stage examined.

Table S1. Primers used

Gene name	Primer name	Primer sequence (5' to 3')	Application
bmpr2a	bmpr2a-3301	TAGGTCTGGCCGAGCGGATTGG	sgRNA
	bmpr2a-3302	AAACCCAATCCGCTCGGCCAGA	
bmpr2b	bmpr2b-3345	TAGGACATCAGTACTGTCACTC	
	bmpr2b-3346	AAACGAGTGACAGTACTGATGT	
amh	amh_2039	AGGCAAGATTTGGGCTGATG	HRMA
	amh_2040	CTTCGGGTTGTTGTCCTGC	
bmpr2a	bmpr2a-3303	CAGAGTGAGCAGAGGGAGTGT	
	bmpr2a-3304	CAGCGGTGTCCTTGATAACAG	
bmpr2b	bmpr2b-3347	GAATCCATCCAGAAGCGGCA	
	bmpr2b-3348	GGGGTATATTTACCGGCCACA	
fshb	fshb_176	CAGATGAGGATGCGTGTGC	Real-time qPCR
	fshb_177	ACCCCTGCAGGACAGCC	
cyp19a1a	cyp19a1a_818	TGTGCGTGTCTGGATCAATGG	
	cyp19a1a_819	AAGCCCTGGACCTGTGAGAG	
inhbaa	inhbaa-931	AACAGGCAGAACAGACGGAGATC	
	inhbaa-932	GCAGCCGAATGTTGACGTTAGC	
ef1a	ef1a_728	GGCTGACTGTGCTGTGCTGATTG	
	ef1a_729	CTTGTCGGTGGGACGGCTAGG	

Supplemental Figures and Tables

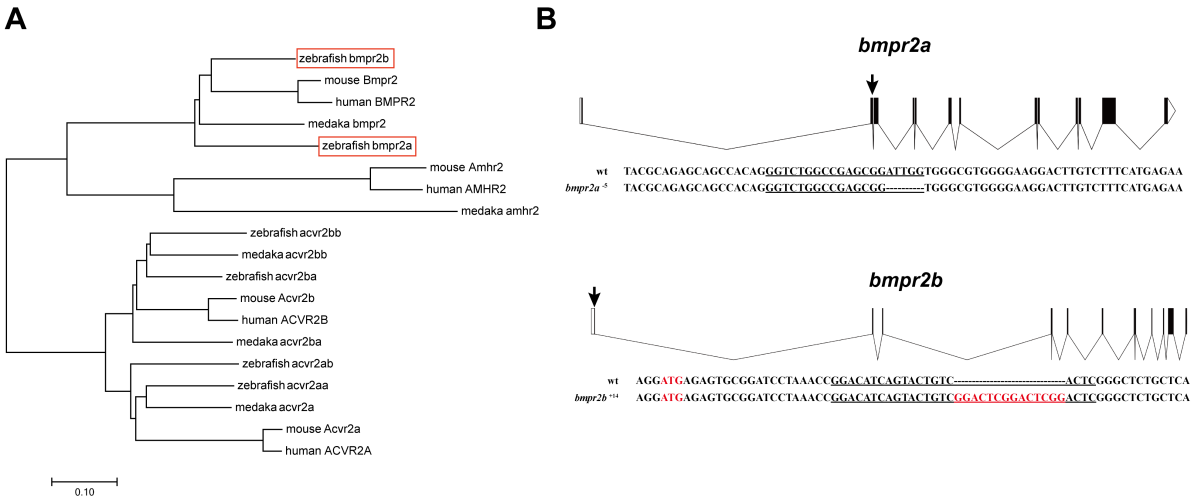

Fig. S1. Bmpr2 receptors (*bmpr2a* and *bmpr2b*) in zebrafish

(A) Phylogenetic analysis of zebrafish *bmpr2a* and *bmpr2b*. The sequences were obtained from Genbank and Ensemble databases. Sequence alignment and tree construction were performed by MEGA software using Neighbor-Joining method. (B) Schematic illustration of CRISPR targeting sites of *bmpr2a* and *bmpr2b* in zebrafish. The arrows indicate the location of targeting sites. Open and solid boxes indicate untranslated and coding exons respectively. Sequences underlined indicate the CRISPR targeting sites and the underlined sequences in red are inserted bases.

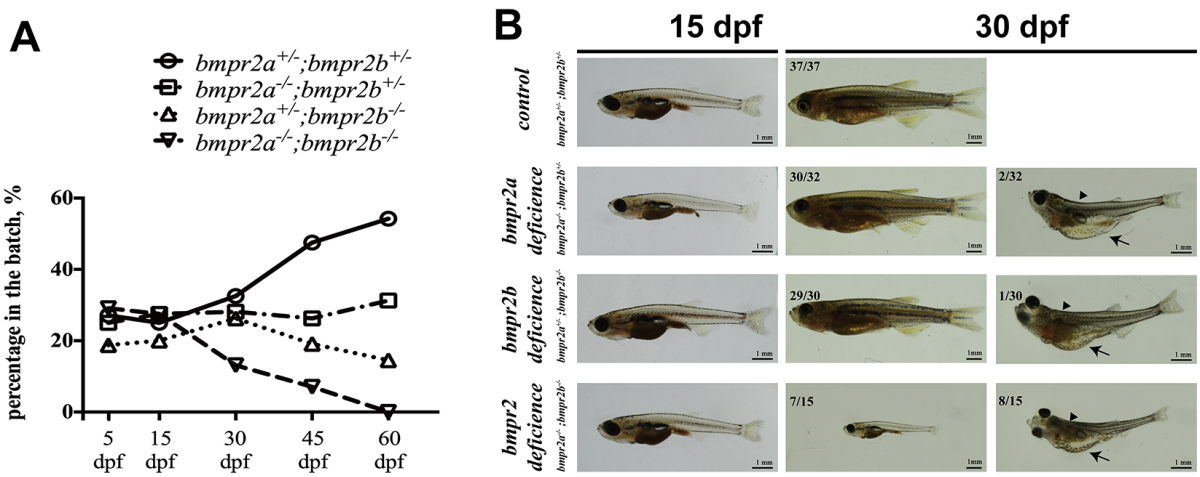

Fig. S2. Bmpr2 deficiency leads to severe developmental defects

The female *bmp2a*$^{-/-}$;*bmpr2b*$^{+/-}$ was crossed with male *bmp2a*$^{+/-}$;*bmpr2b*$^{-/-}$ to produce the offspring with theoretical ratios 1:1:1:1 for different genotypes. The offspring were sampled at different time points (5-60 dpf) for genotyping (A). No obvious abnormalities were observed before 15 dpf among the four genotypes: wild type control (*bmp2a*$^{+/-}$;*bmpr2b*$^{+/-}$), single mutants (*bmp2a*$^{-/-}$;*bmpr2b*$^{+/-}$ and *bmpr2b*$^{+/-}$;*bmpr2b*$^{-/-}$) and double mutant (*bmp2a*$^{-/-}$;*bmpr2b*$^{-/-}$) in terms of survival rate, morphology and growth. However, a significant mortality was observed in the *bmpr2*-deficient double mutant at 30 dpf. The double mutant individuals (*bmp2a*$^{-/-}$;*bmpr2b*$^{-/-}$) that survived at this age all showed obvious developmental defects including edematous abdominal cavity (8 out of 15) and retarded body growth with much smaller body size (7/15) (B). From 30 to 60 dpf, the ratio of double mutant continued to decrease progressively; however, the ratios of the wild type and single mutants did not increase proportionally with the wild type steadily increasing while the single mutants remaining relative constant.

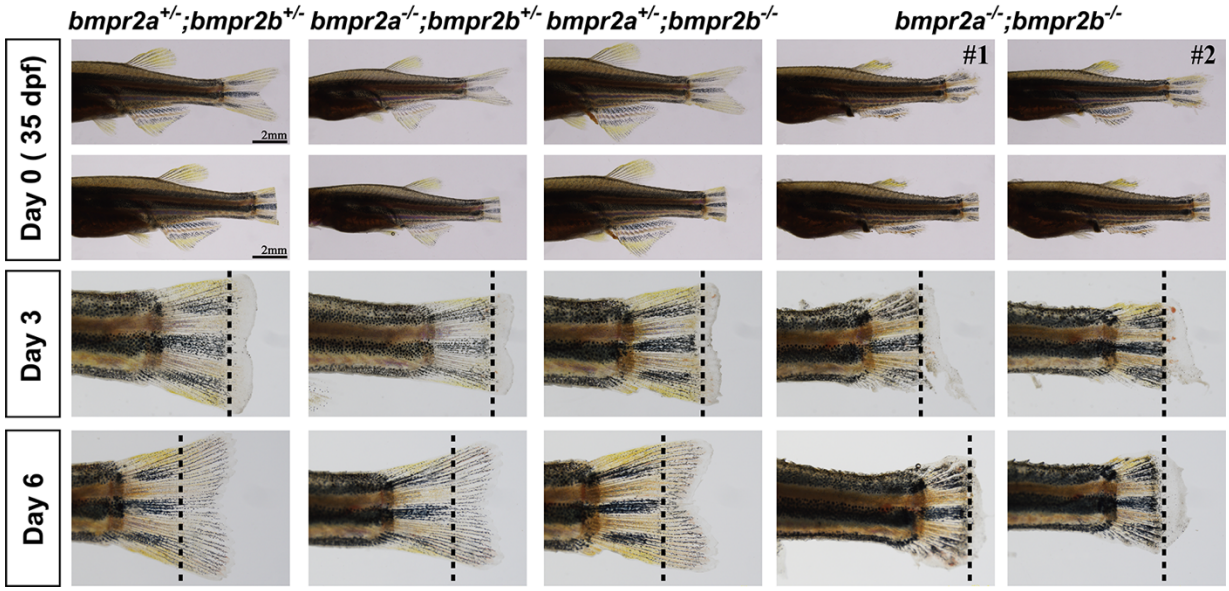

Fig. S3. Defective fin regeneration due to *bmpr2* deficiency

In addition to abdominal edema and retarded growth, some survived double mutants showed abnormal morphology of caudal fin at 35 dpf. To further confirm the role of *bmpr2* signaling in fin development, we performed a caudal fin regeneration assay by amputating the caudal fins at 35 dpf. The dotted line indicates the initial amputation plane. The double mutants (*bmpr2a*$^{-/-}$;*bmpr2b*$^{-/-}$) displayed a quick regeneration with epidermal outgrowth beyond the amputation plane, similar to the single mutants (*bmpr2a*$^{-/-}$;*bmpr2b*$^{+/-}$ and (*bmpr2a*$^{+/-}$;*bmprb2*$^{-/-}$) and control (*bmpr2a*$^{+/-}$;*bmpr2b*$^{+/-}$) at 3 days post amputation (dpa). At 6 dpa, the control and single mutants had fully regenerated the caudal fins with fin rays well developed and tail fork well formed; in contrast, the regeneration of the caudal fins in the double mutants remained unchanged as compared to that at 3 dpa and the regenerated region was covered by the epidermis only without fin rays. The data suggested that *bmpr2* signaling was essential for maintaining normal fin morphology and promoting fin regeneration, and that Bmpr2a and Bmpr2b could functionally compensate for each other in this regard.

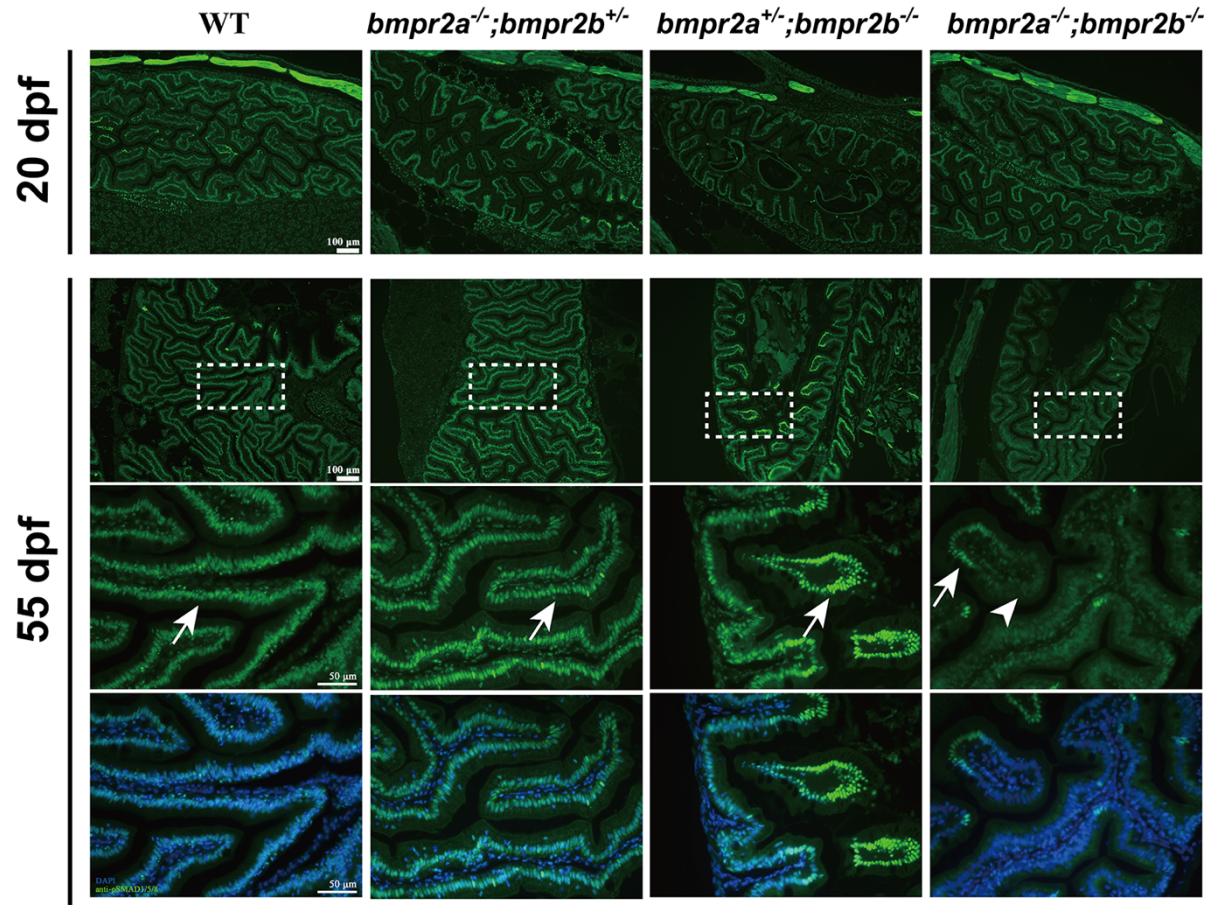

Fig. S4. Bmpr2 deficiency reduces Smad1/5/8 phosphorylation in the intestine

To demonstrate whether the *bmpr2a* and/or *bmpr2b* mutation disrupts BMP signaling activity, we examined the phosphorylation of Smad1/5/8 by immunofluorescent staining for the signal of phosphor-Smad1/5/8 (pSmad1/5/8). At 20 dpf, a strong pSmad1/5/8 signal was observed in the intestines of all genotypes including control (WT), *bmpr2a* and *bmpr2b* single mutants (*bmpr2a*$^{-/-}$;*bmpr2b*$^{+/-}$ and *bmpr2a*$^{+/-}$;*bmpr2b*$^{-/-}$), and the *bmpr2a*-deficient double mutant (*bmpr2a*$^{-/-}$;*bmpr2b*$^{-/-}$). At 55 dpf, the pSmad1/5/8 signal remained strong in the intestinal epithelial cells in control and single mutants (arrows); however, the signal was absent in most of the epithelium cells of the *bmpr2*-deficient double mutants (arrowhead). Interestingly, this was the time window when most double mutants died.

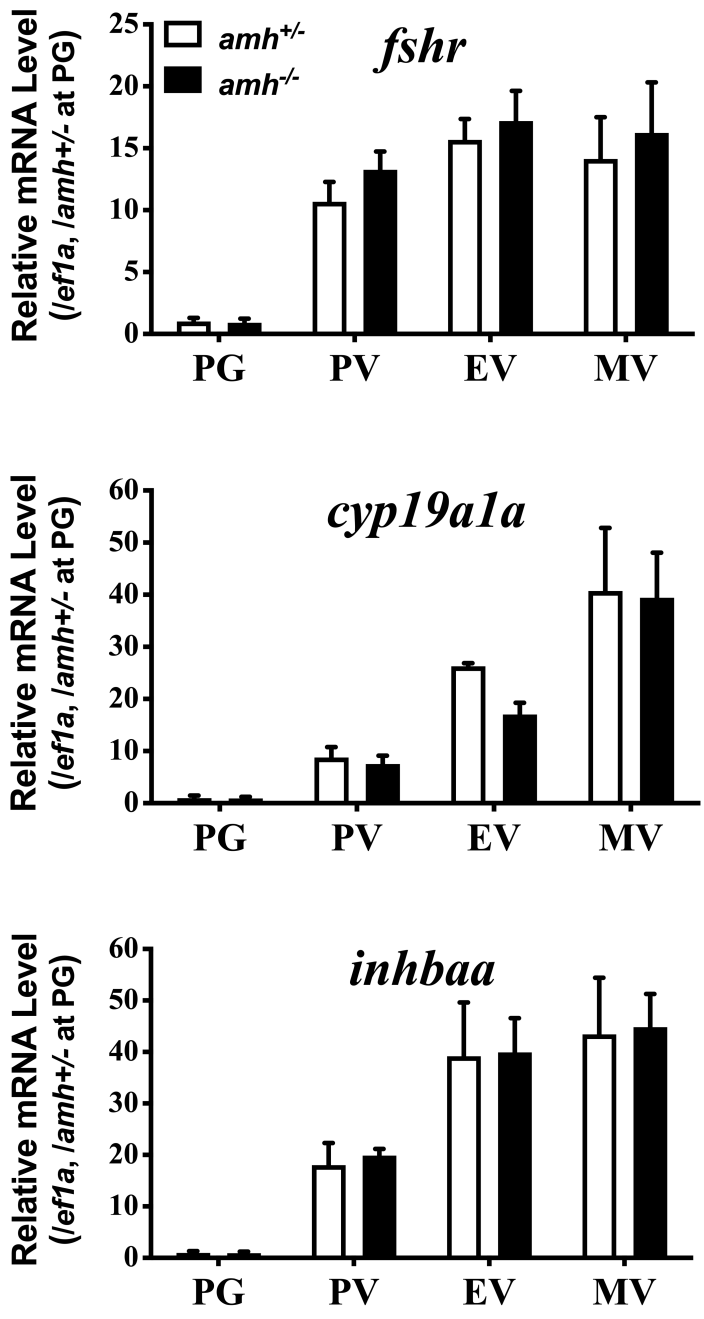

Fig. S5. Expression of *fshr* (FSH receptor), *cyp19a1a* (ovarian aromatase) and *inhbaa* (activin βA) in follicles of *amh* mutant

Follicles of PG (primary growth), PV (pre-vitellogenic), EV (early vitellogenic) and MV (mid-vitellogenic) were isolated from *amh* mutant ($amh^{-/-}$) and control fish ($amh^{+/-}$) for RNA extraction and qPCR quantification. The expression level of each target gene was normalized to the housekeeping gene *ef1a* in the same sample and expressed as the ratio to that of control PG ($amh^{+/-}$). The values are mean ± SEM (n = 3). No significant difference was observed between *amh* mutant and control at any stage examined.

Table S1. Primers used

Gene name	Primer name	Primer sequence (5' to 3')	Application
bmpr2a	bmpr2a-3301	TAGGTCTGGCCGAGCGGATTGG	sgRNA
	bmpr2a-3302	AAACCCAATCCGCTCGGCCAGA	
bmpr2b	bmpr2b-3345	TAGGACATCAGTACTGTCACTC	
	bmpr2b-3346	AAACGAGTGACAGTACTGATGT	
amh	amh_2039	AGGCAAGATTTGGGCTGATG	HRMA
	amh_2040	CTTCGGGTTGTTGTCCTGC	
bmpr2a	bmpr2a-3303	CAGAGTGAGCAGAGGGAGTGT	
	bmpr2a-3304	CAGCGGTGTCCTTGATAACAG	
bmpr2b	bmpr2b-3347	GAATCCATCCAGAAGCGGCA	
	bmpr2b-3348	GGGGTATATTTACCGGCCACA	
fshb	fshb_176	CAGATGAGGATGCGTGTGC	Real-time qPCR
	fshb_177	ACCCCTGCAGGACAGCC	
cyp19a1a	cyp19a1a_818	TGTGCGTGTCTGGATCAATGG	
	cyp19a1a_819	AAGCCCTGGACCTGTGAGAG	
inhbaa	inhbaa-931	AACAGGCAGAACAGACGGAGATC	
	inhbaa-932	GCAGCCGAATGTTGACGTTAGC	
ef1a	ef1a_728	GGCTGACTGTGCTGTGCTGATTG	
	ef1a_729	CTTGTCGGTGGGACGGCTAGG	